$\partial 305 9$

NASA Contractor Report 194893

# Determining the Accuracy of Maximum Likelihood Parameter Estimates With Colored Residuals

Eugene A. Morelli
*Lockheed Engineering & Sciences Company*
*Langley Research Center, Hampton, Virginia*

Vladislav Klein
*The George Washington University*
*Joint Institute for Advancement of Flight Sciences (JIAFS)*
*Langley Research Center, Hampton, Virginia*

National Aeronautics and
Space Administration
Langley Research Center
Hampton, Virginia 23681-0001

N95-11869

Unclas

G3/08    0023058

(NASA-CR-194893) DETERMINING THE
ACCURACY OF MAXIMUM LIKELIHOOD
PARAMETER ESTIMATES WITH COLORED
RESIDUALS (Lockheed Engineering
and Sciences Corp.) 48 p

# Abstract

An important part of building high fidelity mathematical models based on measured data is calculating the accuracy associated with statistical estimates of the model parameters. Indeed, without some idea of the accuracy of parameter estimates, the estimates themselves have limited value. In this work, an expression based on theoretical analysis was developed to properly compute parameter accuracy measures for maximum likelihood estimates with colored residuals. This result is important because experience from the analysis of measured data reveals that the residuals from maximum likelihood estimation are almost always colored. The calculations involved can be appended to conventional maximum likelihood estimation algorithms. Simulated data runs were used to show that the parameter accuracy measures computed with this technique accurately reflect the quality of the parameter estimates from maximum likelihood estimation without the need for analysis of the output residuals in the frequency domain or heuristically determined multiplication factors. The result is general, although the application studied here is maximum likelihood estimation of aerodynamic model parameters from flight test data.

# Nomenclature

| | |
|---|---|
| $a_z$ | vertical acceleration, g units |
| $\mathcal{D}$ | dispersion matrix |
| $E\{\,\cdot\,\}$ | expected value |
| $g$ | gravitational acceleration, 32.174 ft/sec$^2$ |
| $J$ | cost function |
| $K_\alpha$ | upwash correction |
| $L(\,\cdot\,)$ | likelihood function |
| $\mathbf{M}$ | information matrix |
| M | body axis aerodynamic pitching moment, ft-lbf |
| $n_c$ | number of control vector elements |
| $n_o$ | number of output vector elements |
| $n_p$ | number of parameter vector elements |
| $n_s$ | number of state vector elements |
| $N$ | total number of sample times |
| $P(\,\cdot\,)$ | probability distribution |
| $q$ | body axis pitch rate, rad/sec |
| $r_{ii}$ | $i^{\text{th}}$ diagonal element of $\mathbf{R}$ |
| $\mathbf{R}$ | discrete noise covariance matrix |
| $\mathcal{R}_{vv}$ | autocorrelation matrix of $\mathbf{v}$ |
| $\mathbf{S}(i)$ | output sensitivity matrix at time $(i-1)\Delta t$ |
| $t$ | time, sec |
| $T$ | data record length, sec |
| $\mathbf{u}(t)$ | control vector |
| $V$ | airspeed, ft/sec |
| $\mathbf{v}(i)$ | output residual vector at time $(i-1)\Delta t$ |
| $\mathbf{x}(t)$ | state vector |
| $\mathbf{y}(t)$ | output vector |
| $\mathbf{y}(i)$ | output vector at time $(i-1)\Delta t$ |

2

| | |
|---|---|
| $\mathbf{z}(i)$ | measured output at time $(i-1)\Delta t$ |
| $Z$ | body axis aerodynamic vertical force, lbf |
| $\mathbf{Z}$ | the set of $N$ measured output vectors |
| $\alpha$ | angle of attack, rad |
| $\delta_{ij}$ | Kronecker delta |
| $\delta_s$ | stabilator deflection, rad |
| $\Delta t$ | sample time, sec |
| $\theta$ | parameter vector |
| $\nabla_\theta$ | gradient with respect to $\theta$ |
| $\theta_j$ | $j^{\text{th}}$ element of the parameter vector |
| $\sigma_j$ | Cramer-Rao lower bound for the standard error of the $j^{\text{th}}$ parameter |
| $\upsilon(i)$ | noise vector at time $(i-1)\Delta t$ |
| $\mathbf{0}$ | zero vector |

## superscripts

| | |
|---|---|
| $T$ | transpose |
| $\wedge$ | estimate |
| $\cdot$ | time derivative |
| $-1$ | matrix inverse |

## subscripts

| | |
|---|---|
| $m$ | measured |
| $o$ | nominal or trim value |

# I. Introduction

An important part of building high fidelity mathematical models for physical systems is estimating values for the model parameters based on measured data. For the case of aircraft dynamic models, these model parameters generally arise in describing the dependence of aerodynamic forces and moments on state and control variables. Of equal importance with the estimated values of the parameters is their accuracy. This accuracy can be assessed using the Cramer-Rao lower bounds[1], which represent the theoretical minimum variance that is possible for the parameter estimates using an asymptotically unbiased estimator, such as maximum likelihood. Maximum likelihood estimation is also asymptotically efficient, meaning that parameter variances computed for maximum likelihood estimates approach the Cramer-Rao bounds as the number of measured data points increases. References [1]-[3] compare and contrast the Cramer-Rao bound with other methods for assessing the accuracy of parameter estimates. The present work adopts the viewpoint of reference [3] that the Cramer-Rao bound is the best accuracy measure for maximum likelihood parameter estimates.

In this work, the output error formulation of maximum likelihood parameter estimation was used with a fixed linear model structure. This formulation includes measurement noise, but no process noise[4]. The optimization procedure used to determine the maximum likelihood parameter estimates was modified Newton-Raphson[4,5]. In this case, the Cramer-Rao bounds are computed as part of the estimation procedure. It is well known, however, that the Cramer-Rao bounds computed in this way are usually optimistic (too small) compared to the scatter in the parameter estimates from repeated flight test maneuvers[3,6]. This prompted the work of Maine, Iliff and Balakrishnan[3,4,7-9] who traced the discrepancy to the fact that the residuals are colored for real flight test data analysis because output error techniques lump the (unavoidable) deterministic modeling error together with the incoherent part of a measured signal and call this the measurement noise[3]. This results in the measurement noise being colored, because the modeling error generally lies roughly in the same frequency band as the aircraft rigid body dynamics and accounts for a large part of the total noise power. Colored measurement noise impacts parameter estimate accuracy measures, as detailed in references [3],[4],[7]-[9].

The theory underlying the output error formulation of maximum likelihood estimation assumes that the measurement noise is white Gaussian and band limited by the Nyquist frequency. The band limit is the result of discrete measurements taken at the sampling frequency, which is twice the Nyquist frequency. This measurement noise is broad band and incoherent. The term incoherent is meant to imply amplitude discontinuity and a lack of consistent phase-amplitude relationships, causing the autocorrelation function to be close to the impulse function. Heuristically, this part of the residual would be commonly recognized as having no deterministic component. If the structure of the model were correct, the residuals could be expected to be reasonably close to this type of noise. In real flight test data analysis, the

4

residuals inevitably contain deterministic components from such sources as approximations of real aircraft aerodynamic dependencies, unmodeled dynamics such as structural modes, and linearization of the nonlinear equations of motion. References [3], [4], [7]-[9] point out that colored residuals violate the assumptions of conventional maximum likelihood theory and lead to the aforementioned inaccuracy in the Cramer-Rao bounds.

In reference [3], several engineering solutions were proposed to correct for the discrepancy. Each of these solutions was based on the fact that most of the residual power for real flight data analysis is concentrated at relatively low frequencies and is due to deterministic modeling error. This assumption is stretched when relatively high frequency structural modes appear in the data or when the broad band random noise has a large enough magnitude to rival the power of the band limited noise due to modeling error. The solutions offered in reference [3] depend on knowing something about the bandwidth of the dominant source of power in the residuals. Obtaining this information requires Fourier transforms of the residuals and analysis in the frequency domain. The spectra of the residuals depend on the model, the flight condition, the maneuver, and the instrumentation characteristics. All of these factors may change over the course of a flight test program, requiring changes in the corrections for the Cramer-Rao bounds. Finally, all the solutions offered in reference [3] require some engineering judgment, which requires an experienced analyst and limits the quantitative accuracy of the results.

In the present work, a technique was developed which processes the residuals of a conventional maximum likelihood estimation in order to compute quantitatively accurate Cramer-Rao lower bounds for arbitrary residuals. The approach accounts for colored residuals using a simple estimate of the residual correlation. Cramer-Rao lower bounds for the maximum likelihood estimates can be determined automatically and accurately with no heuristic multiplication factors. In addition, existing maximum likelihood estimation routines can be easily upgraded because the technique can be considered a post-processing of the output residuals in order to compute the appropriate Cramer-Rao lower bounds.

The next section contains the theoretical analysis. Following this, the technique was applied in a controlled situation using simulated data. A model of the longitudinal dynamics of a fighter aircraft was used with the true parameter values known. The simulated outputs were corrupted by discrete white Gaussian noise with zero mean. Using ten simulation runs with different realizations of the noise process, it was shown that both the conventional method for computing Cramer-Rao lower bounds and the new technique described in this work produced Cramer-Rao lower bounds representative of the observed scatter in the parameter estimates. Implementation of the new technique was in a subroutine which post-processed the output residuals from the conventional maximum likelihood estimation. Next, the same simulated outputs were corrupted with band limited white noise produced by passing zero mean discrete white Gaussian noise through an 0.5 hz low pass filter and scaling the amplitudes to maintain the same signal to noise

ratio used for the wide band noise cases. Ten different noise sequences were used. In these cases, the Cramer-Rao bounds computed using the conventional method produced optimistic values of the Cramer-Rao lower bounds, in agreement with the results of previous research[3,4,6-9]. The new technique, however, successfully accounted for the band limited residuals and produced quantitatively correct values for the Cramer-Rao lower bounds. Finally, ten different colored noise sequences comprised of a mixture of band limited and wide band noise sequences were generated, again scaling the amplitudes to maintain signal to noise ratio. These colored noise sequences were very similar to residuals observed when analyzing real flight test data. Again, the conventional method gave optimistic Cramer-Rao lower bounds while the new technique produced Cramer-Rao bounds which accurately characterized the scatter in the parameter estimates. This analysis lends confidence in the new technique for future application to determining appropriate Cramer-Rao lower bounds for parameters estimated from flight test data.

# II.  Theoretical Development

A linear model structure for the aircraft dynamics was assumed *a priori* as a result of the small perturbations assumption.  The control inputs were considered perturbations about trim. The model can be represented as

$$\dot{\mathbf{x}}(t) = \mathbf{A}(\theta)\mathbf{x}(t) + \mathbf{B}(\theta)\mathbf{u}(t) \tag{1}$$

$$\mathbf{x}(0) = \mathbf{0} \tag{2}$$

$$\mathbf{y}(t) = \mathbf{C}(\theta)\mathbf{x}(t) + \mathbf{D}(\theta)\mathbf{u}(t) \tag{3}$$

$$\mathbf{z}(i) = \mathbf{y}(i) + \upsilon(i) \qquad i = 1,2,...,N \tag{4}$$

where $\mathbf{x}$ is the $n_s \times 1$ state vector, $\mathbf{u}$ is the $n_c \times 1$ control vector, and $\mathbf{y}$ is the $n_o \times 1$ output vector.  The $n_o \times 1$ measured output vector is represented by $\mathbf{z}(i)$.  The notation $\mathbf{y}(i)$ represents the sampled value of $\mathbf{y}(t)$ at $t=(i-1)\Delta t$.  There are $N$ sampled data points.  For conventional maximum likelihood, the discrete measurement noise vector $\upsilon(i)$ is assumed to be zero mean white Gaussian and band limited at the Nyquist frequency with

$$E\{\upsilon(i)\} = \mathbf{0} \qquad E\{\upsilon(i)\upsilon^T(j)\} = \mathbf{R}\,\delta_{ij} \tag{5}$$

where $\mathbf{R}$ is the discrete noise covariance matrix, $\delta_{ij}$ is the Kronecker delta, and $E$ is the expectation operator.

The maximum likelihood estimate of the parameter vector maximizes the conditional probability of realizing the measurements[4,5]:

$$\hat{\theta} = \arg \max_{\theta} \left[ P(\mathbf{Z}|\theta) \right] \tag{6}$$

where $\mathbf{Z}$ is the set of all measurement vectors, $\mathbf{z}(i)$ for $i=1, 2, ..., N$.  The conditional probability distribution, $P(\mathbf{Z}|\theta)$, is also known as the likelihood function, $L(\theta)$, and is given by

7

$$L(\theta) \equiv P(\mathbf{Z}|\theta) = \frac{1}{\left[(2\pi)^{n_o}|\mathbf{R}|\right]^{N/2}} \exp\left\{-\frac{1}{2}\sum_{i=1}^{N}[\mathbf{z}(i)-\mathbf{y}(i)]^T\mathbf{R}^{-1}[\mathbf{z}(i)-\mathbf{y}(i)]\right\} \qquad (7)$$

Maximizing the likelihood function in equation (7) is equivalent to minimizing its negative logarithm, known as the log likelihood function,

$$-\ln L(\theta) = \frac{1}{2}\sum_{i=1}^{N}[\mathbf{z}(i)-\mathbf{y}(i)]^T\mathbf{R}^{-1}[\mathbf{z}(i)-\mathbf{y}(i)] + \frac{N}{2}\ln|\mathbf{R}| \qquad (8)$$

where the added constant $\frac{n_o N}{2}\ln(2\pi)$ was omitted because it has no effect on the optimization. When $\mathbf{R}$ is known, minimizing the log likelihood function in equation (8) is equivalent to minimizing the cost function

$$J(\theta) = \frac{1}{2}\sum_{i=1}^{N}[\mathbf{z}(i)-\mathbf{y}(i)]^T\mathbf{R}^{-1}[\mathbf{z}(i)-\mathbf{y}(i)] \qquad (9)$$

The cost in equation (9) can be minimized using a modified Newton-Raphson technique to determine parameter updates[5], starting from some initial guess of the parameter vector. The initial guess for the parameter vector can be obtained from equation error methods[6]. When the parameter vector estimate, $\hat{\theta}$, is close to the true parameter vector, $\theta$, the estimated output can be linearized with respect to the parameter vector,

$$\mathbf{y}(i) = \hat{\mathbf{y}}(i) + \frac{\partial \mathbf{y}(i)}{\partial \theta}\bigg|_{\theta=\hat{\theta}}\left(\theta - \hat{\theta}\right) \qquad i = 1, 2, \ldots, N \qquad (10)$$

where $\hat{\mathbf{y}}(i)$ denotes the output vector computed using the estimated parameter vector $\hat{\theta}$ at time $(i-1)\Delta t$. Defining the sensitivity matrix,

$$\mathbf{S}(i) = \frac{\partial \mathbf{y}(i)}{\partial \theta}\bigg|_{\theta=\hat{\theta}} \qquad i = 1, 2, \ldots, N \qquad (11)$$

8

equation (10) becomes

$$y(i) = \hat{y}(i) + S(i)\left(\theta - \hat{\theta}\right) \qquad i = 1, 2, \ldots, N \qquad (12)$$

The $j^{th}$ column of the sensitivity matrix contains the output sensitivities for the $j^{th}$ parameter, $\theta_j$, computed from

$$\frac{d}{dt}\left[\frac{dx}{d\theta_j}\right] = \frac{dA}{d\theta_j}x + A\frac{dx}{d\theta_j} + \frac{dB}{d\theta_j}u \qquad (13)$$

$$\frac{dx}{d\theta_j}(0) = 0 \qquad (14)$$

$$\frac{dy}{d\theta_j} = \frac{dC}{d\theta_j}x + C\frac{dx}{d\theta_j} + \frac{dD}{d\theta_j}u \qquad (15)$$

for $j = 1, 2, \ldots, n_p$, where $n_p$ is the number of parameters. Equations (13)-(15) follow from differentiating equations (1)-(3) with respect to the $\theta_j$, along with the assumed analyticity of $x$.

To minimize the cost function, substitute for $y(i)$ from equation (12) into equation (9) and set the gradient of the cost function with respect to the parameter vector equal to zero,

$$\nabla_\theta J(\theta) = -\sum_{i=1}^{N} S(i)^T R^{-1} \left[z(i) - \hat{y}(i) - S(i)\left(\theta - \hat{\theta}\right)\right] = 0 \qquad (16)$$

Solving for the parameter update gives

$$\Delta\hat{\theta} \equiv \theta - \hat{\theta} = \left[\sum_{i=1}^{N} S(i)^T R^{-1} S(i)\right]^{-1} \sum_{i=1}^{N} S(i)^T R^{-1} \left[z(i) - \hat{y}(i)\right] \qquad (17)$$

9

Equation (17) gives the modified Newton-Raphson step which is added to a current estimate of the parameter vector in order to approach the true value of the parameter vector. The "modified Newton-Raphson" name arises from the fact that equation (17) can also be found by expanding the cost function to second order in terms of $\Delta\hat{\theta}$, and using a conventional Newton-Raphson optimization with part of the second order gradient term dropped (see reference [5] for details). In practice, there are times when the modified Newton-Raphson step computed from equation (17) leads to an increase in the cost function or a divergence. This is because the Newton-Raphson step assumes that the current estimate of the parameter vector is near the true value. Using several iterations of a simplex algorithm[10] when the Newton-Raphson step produces an increase in the cost was found to be very effective. This approach was followed in the present study and makes the optimization divergence proof. If measured outputs are used instead of computed outputs to force the sensitivity equations in the first calculation of the modified Newton-Raphson step (see reference [5] for details), the solution of the maximum likelihood estimation problem becomes insensitive to initial parameter estimates and it is not necessary to use equation error methods to determine good starting values for the parameters. This technique was used for all maximum likelihood estimation in the present work.

When repeated application of equation (17) converges, an estimate of the measurement noise covariance matrix, **R**, can be obtained from the output residuals. The expression for the estimate of **R** comes from taking the derivative of the right hand side of equation (8) with respect to **R**, setting the result equal to zero, and solving for **R**,

$$\hat{\mathbf{R}} = \frac{1}{N} \sum_{i=1}^{N} \left[ \mathbf{z}(i) - \mathbf{y}(i) \right] \left[ \mathbf{z}(i) - \mathbf{y}(i) \right]^{T} \tag{18}$$

Often only the diagonal elements of the **R** matrix are estimated from equation (18), enforcing an assumption that the measurement noise sequences for the $n_o$ measured outputs are uncorrelated with one another. This assumption is generally a good one for real flight test data. All estimates of the measurement noise covariance matrix in this work assume a diagonal $\hat{\mathbf{R}}$ matrix. Retaining the full $\hat{\mathbf{R}}$ matrix could have been done with little conceptual difficulty, but the expected gains did not warrant the extra computation involved. The noise covariance matrix estimate, $\hat{\mathbf{R}}$, was used in the cost function of equation (9), and the minimization process described above for known **R** was repeated. Thus, the maximum likelihood estimation proceeds by alternately estimating the noise covariance matrix from equation (18) and minimizing the cost function using equation (17) with the latest value of the estimated noise covariance matrix. Convergence is reached when the estimated parameter vector, $\hat{\theta}$, the estimated noise covariance matrix, $\hat{\mathbf{R}}$, and the cost, $J(\hat{\theta})$, reach nearly constant values. Since maximum likelihood

10

estimation is asymptotically unbiased[4], the estimated parameter vector, $\hat{\theta}$, should be close to the true value, $\theta$, and the gradient of the cost function with respect to the parameter vector should be close to zero. From equation (16),

$$\nabla_{\theta} J(\theta)\big|_{\theta=\hat{\theta}} \approx -\sum_{i=1}^{N} S(i)^T R^{-1} \left[ z(i) - \hat{y}(i) \right] \approx 0 \qquad (19)$$

For practical computation, simultaneous satisfaction of the numerical criteria given below were used to define convergence of the maximum likelihood estimation:

$$\left| \left[ \hat{\theta}_j \right]_k - \left[ \hat{\theta}_j \right]_{k-1} \right| < 1.0 \times 10^{-5} \quad \forall \, j, \quad j = 1, 2, \dots, n_p$$

$$\left| \frac{\left[ \hat{r}_{ii} \right]_k - \left[ \hat{r}_{ii} \right]_{k-1}}{\left[ \hat{r}_{ii} \right]_{k-1}} \right| < 0.05 \quad \forall \, i, \quad i = 1, 2, \dots, n_o$$

$$\left| \frac{J\left( \hat{\theta}_k \right) - J\left( \hat{\theta}_{k-1} \right)}{J\left( \hat{\theta}_{k-1} \right)} \right| < 0.001 \qquad (20)$$

$$\left| \frac{\partial J(\theta)}{\partial \theta_j} \right|_{\theta=\hat{\theta}} < 0.05 \quad \forall \, j, \quad j = 1, 2, \dots, n_p$$

where $k$ denotes the current estimate iteration number and $\hat{r}_{ii}$ denotes the estimate of the $i^{th}$ diagonal element of the discrete measurement noise covariance matrix. The approximate expression for the cost gradient with respect to the parameters (equation (19)) was used for the last criterion in (20).

The minimum achievable parameter variances using an asymptotically unbiased and efficient estimator, such as maximum likelihood, are called the Cramer-Rao lower bounds and are given by the diagonal elements of the dispersion matrix, $\mathcal{D}$[3-5]. This dispersion matrix is defined as the inverse of the information matrix $M$, the latter being a measure of the information contained in the data from an experiment. The expressions for theses matrices are[3,4]

$$M = \sum_{i=1}^{N} S(i)^T R^{-1} S(i) \qquad (21)$$

11

$$\mathcal{D} = \mathbf{M}^{-1} = \left[ \sum_{i=1}^{N} \mathbf{S}(i)^{T} \mathbf{R}^{-1} \mathbf{S}(i) \right]^{-1} \tag{22}$$

The square root of the $j^{th}$ diagonal element of $\mathcal{D}$, $d_{jj}$, gives the Cramer-Rao lower bound for the standard error of the $j^{th}$ parameter,

$$\sigma_j = \sqrt{d_{jj}} \qquad j = 1, 2, \ldots, n_p \tag{23}$$

It can be seen from equations (17) and (22) that the dispersion matrix is computed when determining the modified Newton-Raphson step as part of the conventional maximum likelihood estimation. The assumption that the output residuals are white and therefore uncorrelated in time is implicit in the algorithm and indicated in equation (5). The next section details the theory involved in accounting for arbitrary colored output residuals, which are correlated in time.

When the conventional maximum likelihood estimation has converged, the estimated parameter vector will be close to the true value and equation (17) holds. Define the residual vector

$$\mathbf{v}(i) \equiv \mathbf{z}(i) - \hat{\mathbf{y}}(i) \qquad i = 1, 2, \ldots, N \tag{24}$$

The estimated parameter covariance matrix can be expressed using equation (17) with substitutions from the definitions in equations (22) and (24),

$$E\left\{ \left( \hat{\theta} - \theta \right) \left( \hat{\theta} - \theta \right)^{T} \right\} = E\left\{ \sum_{i=1}^{N} \sum_{j=1}^{N} \mathcal{D} \mathbf{S}(i)^{T} \mathbf{R}^{-1} \mathbf{v}(i) \mathbf{v}(j)^{T} \mathbf{R}^{-1} \mathbf{S}(j) \mathcal{D} \right\} \tag{25}$$

The dispersion matrix, the discrete noise covariance matrix inverse and the sensitivities in equation (25) are from the conventional maximum likelihood estimation. If it is assumed that the dependence of these quantities on the parameter vector estimate is small at the maximum likelihood solution, the estimated parameter covariance matrix can be written as

$$E\left\{\left(\hat{\theta}-\theta\right)\left(\hat{\theta}-\theta\right)^T\right\} = \mathcal{D}\left[\sum_{i=1}^{N}\sum_{j=1}^{N} S(i)^T \mathbf{R}^{-1} E\left\{\mathbf{v}(i)\mathbf{v}(j)^T\right\} \mathbf{R}^{-1} S(j)\right]\mathcal{D} \qquad (26)$$

When the output residuals are assumed to be zero mean white (see equation (5)), then

$$E\left\{\mathbf{v}(i)\mathbf{v}(j)^T\right\} = \mathbf{R}\,\delta_{ij} \qquad (27)$$

From equations (22), (26) and (27) it is easy to see that the parameter vector covariance matrix reduces to the dispersion matrix, $\mathcal{D}$, when the output residuals are white. For colored residuals, the estimated parameter covariance matrix can be computed from equation (26) using an estimated value for $E\left\{\mathbf{v}(i)\mathbf{v}(j)^T\right\}$. Define the discrete autocorrelation of the output residuals,

$$\mathfrak{R}_{\mathbf{vv}}(k) \equiv \frac{1}{N}\sum_{i=1}^{N} \mathbf{v}(i)\mathbf{v}(i+k)^T = \mathfrak{R}_{\mathbf{vv}}(-k) \qquad (28)$$

where $\mathbf{v}$ is assumed to be periodic, so that $\mathbf{v}(N+1)=\mathbf{v}(1)$, $\mathbf{v}(N+2)=\mathbf{v}(2)$, etc. It follows that

$$E\left\{\mathbf{v}(i)\mathbf{v}(j)^T\right\} = \mathfrak{R}_{\mathbf{vv}}(i-j) \qquad (29)$$

Substituting equation (29) into equation (26),

$$E\left\{\left(\hat{\theta}-\theta\right)\left(\hat{\theta}-\theta\right)^T\right\} = \mathcal{D}\left[\sum_{i=1}^{N} S(i)^T \mathbf{R}^{-1}\sum_{j=1}^{N} \mathfrak{R}_{\mathbf{vv}}(i-j)\,\mathbf{R}^{-1} S(j)\right]\mathcal{D} \qquad (30)$$

Setting $k = i - j$, equation (30) can be written as

$$E\left\{\left(\hat{\theta}-\theta\right)\left(\hat{\theta}-\theta\right)^T\right\} = \mathcal{D}\left[\sum_{i=1}^{N} S(i)^T \mathbf{R}^{-1}\left(\sum_{k=i-N}^{i-1} \mathfrak{R}_{\mathbf{vv}}(k)\,\mathbf{R}^{-1} S(i-k)\right)\right]\mathcal{D} \qquad (31)$$

13

Equation (31) was used to account for colored residuals, which are correlated in time. The dispersion matrix, $\mathcal{D}$, the estimated noise covariance matrix inverse, $\mathbf{R}^{-1}$, and the sensitivities, $\mathbf{S}$, are from the conventional maximum likelihood estimation. Equations (28) and (31) embody the required post-processing applied to a conventional maximum likelihood solution to account for colored residuals.

For unbiased parameter estimates, the Cramer-Rao inequality can be stated in general form as

$$E\left\{\left(\hat{\theta}-\theta\right)\left(\hat{\theta}-\theta\right)^{T}\right\} \geq \left[-E\left\{\nabla_{\theta}^{2} \ln P\left(\mathbf{Z}|\theta\right)\right\}\right]^{-1} \tag{32}$$

When the discrete measurement noise is white out to the Nyquist frequency with known covariance, substituting for $P\left(\mathbf{Z}\,|\,\theta\right)$ from equation (7) makes the right side of inequality (32) equal to the dispersion matrix (cf. equation (22)).

If the colored noise sequence representing the residuals is assumed to be caused by modeling error, then the maximum likelihood parameter estimates are biased, so that

$$E\left\{\hat{\theta}\right\} = \theta + \mathbf{b}(\theta) \tag{33}$$

where $\mathbf{b}(\theta)$ is a vector of bias errors which are unknown and unknowable in practice. For the biased parameter estimates, the right side of inequality (32) will include additional terms where the elements of the dispersion matrix will be multiplied by $\nabla_{\theta}\mathbf{b}(\theta)$ and $\left[\nabla_{\theta}\mathbf{b}(\theta)\right]\left[\nabla_{\theta}\mathbf{b}(\theta)\right]^{T}$ (see reference [3] for details). In the present analysis, the deterministic modeling error is included in the measurement noise, making the residuals colored. The approach taken here for arbitrary frequency content in the measurement noise could then be viewed as effectively including the bias error due to deterministic modeling error as part of the parameter accuracy measure which accounts for colored residuals.

# IV.  Results

The longitudinal short period dynamics of the F-18 High Angle of Attack Research Vehicle (HARV) fighter aircraft at approximately 20 degrees angle of attack and an altitude of 25,000 feet were simulated for this study.  The model was

$$
\begin{bmatrix} \dot{\alpha}(t) \\ \dot{q}(t) \end{bmatrix} = \begin{bmatrix} Z_\alpha & 1+Z_q \\ M_\alpha & M_q \end{bmatrix} \begin{bmatrix} \alpha(t) \\ q(t) \end{bmatrix} + \begin{bmatrix} Z_{\delta_s} & Z_o \\ M_{\delta_s} & M_o \end{bmatrix} \begin{bmatrix} \delta_s(t) \\ 1 \end{bmatrix}
\tag{34}
$$

$$
\begin{bmatrix} \alpha(0) \\ q(0) \end{bmatrix} = \begin{bmatrix} 0 \\ 0 \end{bmatrix}
\tag{35}
$$

$$
\begin{bmatrix} \alpha_c(t) \\ q(t) \\ a_z(t) \end{bmatrix} = \begin{bmatrix} K_\alpha & 0 \\ 0 & 1 \\ \dfrac{V_o Z_\alpha}{g} & \dfrac{V_o Z_q}{g} \end{bmatrix} \begin{bmatrix} \alpha(t) \\ q(t) \end{bmatrix} + \begin{bmatrix} 0 & 0 \\ 0 & 0 \\ \dfrac{V_o Z_{\delta_s}}{g} & a_{z_o} \end{bmatrix} \begin{bmatrix} \delta_s(t) \\ 1 \end{bmatrix}
\tag{36}
$$

$$
\begin{bmatrix} \alpha_m(i) \\ q_m(i) \\ a_{z_m}(i) \end{bmatrix} = \begin{bmatrix} \alpha_c(i) \\ q(i) \\ a_z(i) \end{bmatrix} + \begin{bmatrix} \upsilon_1(i) \\ \upsilon_2(i) \\ \upsilon_3(i) \end{bmatrix}
\tag{37}
$$

The input was symmetric stabilator deflection in radians ($\delta_s$), and the measured output quantities were angle of attack in radians ($\alpha_m$), pitch rate in radians per second ($q_m$), and vertical acceleration in g units ($a_{z_m}$).

To assess the performance of the new technique for computing Cramer-Rao bounds, thirty simulation runs were made using various measurement noise processes.  Maximum likelihood estimation as described in the previous section was used to estimate the parameters.  Since the true parameter values were known for the simulation data, the true accuracy of the maximum likelihood estimates could be compared to that indicated by the conventional calculation of the Cramer-Rao bounds (equations (18) and (22)) and the alternate calculation accounting for arbitrary frequency content in the residuals (equation (31)).

15

To make the simulation runs realistic, the stabilator input was taken from measured data for the F-18 HARV flying a maneuver designed specifically for accurate parameter estimation[11]. The stabilator input is shown in figure 1. In addition, the true values of the parameters (given in column 2 of Table 1) approximately reflect the short period dynamics of the F-18 HARV at 20 degrees angle of attack and an altitude of 25,000 feet. The stabilator input and true parameter values were the same for each simulated data run, so that the information in the data was constant. The sampling rate was 50 hz and the time length was 14 seconds. Standard errors from the Cramer-Rao bounds computed using the conventional computation come from the square root of the diagonal elements of matrix $\mathcal{D}$ in equation (22), with $\mathbf{R}$ estimated from equation (18). The standard errors based on the Cramer-Rao bounds corrected for colored residuals are the square root of the diagonal elements of the matrix computed by equation (31). Results from both the conventional computation and the corrected calculation were expressed in terms of the ratio of the absolute deviation of each parameter estimate from its true value to the computed standard error from the Cramer-Rao bound, $\left|\hat{\theta}_j - \theta_j\right|/\sigma_j$, for $j=1,2,...,n_p$. For any given maneuver, only the denominator of this ratio was different for the conventional versus corrected calculations of the Cramer-Rao bounds. For a maximum likelihood estimator, the probability distribution of the parameter estimates about their true value approaches a Gaussian distribution as the number of data points gets large. Therefore, these ratios should be less than 3 almost all the time if the computed Cramer-Rao bounds reflect the true accuracy of the estimates.

For the first ten simulation runs, the added measurement noise was zero mean white Gaussian, with standard deviations set to one fifth the root mean square of each uncorrupted output. This made all signal to noise ratios approximately 5 to 1. Typical simulated measured outputs are shown in figure 2, from run 1. Figure 3 shows a typical noise sequence. Noise power was uniform over the entire frequency band out to the Nyquist frequency, 25 hz, as shown in the noise power spectrum of figure 4.

Tables 1 through 10 contain the results from the maximum likelihood estimation using simulated data runs 1 through 10, respectively. The values in the last two columns of each table are the ratio of true parameter estimate accuracy to the computed Cramer-Rao bounds for the standard errors. Measurement noise power was evenly distributed up to the Nyquist frequency for each of these cases. Nearly all values in the last two columns of tables 1 through 10 were less than 3, indicating that both the conventional and the corrected Cramer-Rao bounds accurately reflected the true parameter estimation accuracy. Figures 5 and 6 depict typical results for one parameter, $Z_\alpha$, for these 10 runs. The error bars represent the Cramer-Rao bounds for the standard errors computed using the conventional calculation for figure 5 and the corrected calculation for figure 6. The error bars in both plots accurately reflect the scatter of the parameter estimates. The harmony between the Cramer-Rao bounds and the scatter in the estimates indicates that there is sufficient information in the data and that the length of the data records is

16

sufficient for the true accuracy of the parameter estimates to closely approach the Cramer-Rao bounds.

For simulation runs 11 through 20, the random measurement noise power was limited to frequencies between 0 hz and 0.5 hz, inclusive. This frequency band corresponds roughly to the bandwidth of the uncorrupted simulated outputs. Figure 7 shows typical simulated measured outputs which have been corrupted by the band limited noise, from run 11. The noise sequence was generated by passing zero mean white Gaussian noise through a fifth order Chebyshev low pass filter with frequency cutoff set at 0.5 hz, then scaling the resulting band limited noise to achieve the same 5 to 1 signal to noise ratio used for the other simulation runs. Figure 8 shows a typical band limited noise sequence. Figure 9 is the corresponding power spectrum, showing essentially no components above 0.5 hz.

Tables 11 through 20 contain the results from the maximum likelihood estimation using the simulated data runs 11 through 20, respectively. The data in these tables show that the conventional calculation for the Cramer-Rao bounds frequently gave values that were too small (see the fourth column of each table). In contrast, the last column of each table indicates that the corrected calculation for the Cramer-Rao bounds has properly accounted for the change in the residual spectra, since these values rarely exceed 3.

Figures 10 and 11 depict the results for one parameter, $Z_\alpha$, for these 10 runs. The error bars represent the Cramer-Rao bounds for the standard errors computed using the conventional calculation for figure 10 and the corrected calculation for figure 11. These plots show that the standard calculation for the Cramer-Rao bounds gave optimistic values, whereas the corrected calculation for the Cramer-Rao bounds automatically produced Cramer-Rao bounds which accurately reflect the scatter of the estimates. Results for other parameters were similar to those plotted in figures 10 and 11 for $Z_\alpha$.

It was not necessary to supply information about the bandwidth of the dominant power in the residuals to the algorithm for corrected Cramer-Rao bounds because this information was incorporated automatically via the autocorrelation function appearing in equation (31). Thus, the algorithm should work for arbitrary residual spectra. This attribute can be important when the colored measurement noise includes significant power from unmodeled structural modes, whose frequency content is generally higher than that of the rigid body dynamics.

For simulation runs 21 through 30, ten different colored noise sequences were used with the same uncorrupted simulation outputs. Each noise sequence had 90% of its power in the frequencies between 0 hz and 0.5 hz inclusive, with the remaining power taken by white Gaussian noise out to the Nyquist frequency. The noise sequences were thus a combination of the two types of noise used previously. Figure 12 shows typical simulated measured outputs which have been corrupted by the colored noise, from run 21. This type of noise is quite close to the residual sequences observed when analyzing real flight test data, and was chosen for that

reason. The band limited part of the noise sequence was generated in the same manner as before, and the resulting colored noise sequences were scaled to maintain the same 5 to 1 signal to noise ratio used in the other simulation runs. Figure 13 shows a typical colored noise sequence. Figure 14 is the colored noise power spectrum, showing most of the power below 0.5 hz, with some small components out to the Nyquist frequency, 25 hz. The vertical scale for figure 14 is logarithmic so that the relatively small high frequency components can be seen.

Tables 21 through 30 contain the results from the maximum likelihood estimation using the simulated data runs 21 through 30, respectively. As in the case of narrow band limited noise, the data in these tables show that the conventional calculation for the Cramer-Rao bounds frequently gave optimistic values for the parameter accuracies. The last column of each table indicates that the corrected calculation for the Cramer-Rao bounds again properly accounted for the change in the residual spectra. As before, the values in the last column of each table rarely exceed 3. Additional runs (results not shown) were made with various residual power spectra, including some runs where residuals from flight test data analysis were added to the uncorrupted simulated outputs. Results from all these cases were very similar to those presented in tables 11-30.

Figures 15 and 16 depict the results for one parameter, $Z_\alpha$, for the 10 colored noise runs. The error bars represent the Cramer-Rao bounds for the standard errors computed using the conventional calculation for figure 15 and the corrected calculation for figure 16. Results for other parameters were similar to those plotted in figures 15 and 16. From these plots, and in general from the last two columns of tables 11-30, it is clear that the conventional calculation for the Cramer-Rao bounds gave optimistic values for the Cramer-Rao bounds when the residual spectrum was not white out to the Nyquist frequency. This is in agreement with previous research[3,4,8,9]. In addition, the extent to which the conventional Cramer-Rao bounds misrepresented the true parameter accuracy was neither consistent nor predictable from parameter to parameter or from run to run. This phenomena has been observed previously when analyzing flight test data from repeated maneuvers[6]. It follows that the common practice of applying a fixed correction factor to the conventional calculation of the Cramer-Rao bounds is incorrect to a varying and unpredictable degree in cases where the residual spectrum is colored by modeling error in the frequency band of the system dynamics. The corrected calculation for the Cramer-Rao bounds presented here produced consistently accurate measures of the scatter in the parameter estimates, using an algorithm with moderate computational cost that can be applied as a post-processing of the output residuals from a conventional maximum likelihood solution.

18

# V.   Concluding Remarks

Algorithms for aircraft parameter estimation using the output error formulation of maximum likelihood are in widespread use.  Current practice for determining the accuracy of such estimates calls for use of a correction factor to account for the fact that the output residuals from real flight test data analysis are virtually never white out to the Nyquist frequency, as assumed in the conventional theory, but rather are colored, with most of the power in a frequency band similar to that of the system dynamics.  Such an approach is shown here to be inadequate if a quantitative measure of the accuracy of the parameter estimates is desired.  In this work, an expression based on theoretical analysis was developed to compute parameter accuracy measures for maximum likelihood estimates with colored residuals.  This result is important because the residuals from maximum likelihood estimation are almost always colored in practice, due to unmodeled dynamics in the real physical system.  At a more general level, the utility of the parameter estimates is limited when there is no firm idea of the accuracy of the estimates.

The calculations involved in the algorithm for computing Cramer-Rao bounds that account for colored residuals can be carried out in a short subroutine called at the conclusion of a conventional maximum likelihood estimation algorithm.  This approach was used to generate the results in this report.  Bandwidth of the dominant power in the residuals need not be known or estimated, as it is accounted for automatically in the algorithm.  In addition, there is no need for heuristic correction factors.  The algorithm works for arbitrary residual spectra and all calculations are performed in the time domain.  This obviates the need for any frequency domain analysis of the residuals.

Simulated data runs using various noise sequences were carried out to demonstrate the performance of the algorithm in computing the Cramer-Rao bounds.  This analysis showed that the algorithm developed in this work is a simple, accurate, and generally applicable technique for quantitative determination of the quality of parameter estimates for the output error formulation of maximum likelihood estimation.

# VI.   Acknowledgments

# VII. References

1. Murphy, P.C., "A Methodology for Airplane Parameter Estimation and Confidence Interval Determination in Nonlinear Estimation Problems", NASA RP 1153, April 1986.

2. Murphy, P.C., "Efficient Computation of Confidence Intervals of Parameters", AIAA paper 87-2624-CP, Atmospheric Flight Mechanics Conference, Monterey, California, August 1987 (also NASA Tech Brief LAR-14341).

3. Maine, R.E. and Iliff, K.W., "The Theory and Practice of Estimating the Accuracy of Dynamic Flight-Determined Coefficients", NASA RP 1077, July 1981.

4. Maine, R.E. and Iliff, K.W., "Application of Parameter Estimation to Aircraft Stability and Control - The Output-Error Approach", NASA RP 1168, June 1986.

5. Taylor, L.W., Jr. and Iliff, K.W. "Systems Identification using a Modified Newton-Raphson Method - A FORTRAN Program", NASA TN D-6734, May 1972.

6. Klein, V., "Determination of Stability and Control Parameters of a Light Airplane from Flight Data using Two Estimation Methods", NASA TP-1306, March 1979.

7. Iliff, K.W. and Maine, R.E., "Further Observations on Maximum Likelihood Estimates of Stability and Control Characteristics Obtained from Flight Data", AIAA paper 77-1133, Atmospheric Flight Mechanics Conference, Hollywood, Florida, August 1977.

8. Maine, R.E. and Iliff, K.W., "Use of Cramer-Rao Bounds on Flight Data with Colored Residuals", *Journal of Guidance and Control*, Vol. 4, No. 2, March-April 1981.

9. Balakrishnan, A.V. and Maine, R.E., "Improvements in Aircraft Extraction Programs", NASA CR 145090, 1975.

10. Press, W.H., et al., *Numerical Recipes (FORTRAN version)*, Cambridge University Press, New York, NY, 1989.

11. Morelli, E.A., "Practical Input Optimization for Aircraft Parameter Estimation Experiments", NASA CR 191462, May 1993.

**Table 1** LONGITUDINAL DYNAMIC MODEL PARAMETER ESTIMATES AND CRAMER-RAO BOUNDS - RUN 1 (white noise)

| Parameter | True Value, $\theta$ | Estimate, $\hat{\theta}$ | $\left\| \dfrac{\hat{\theta} - \theta}{\text{standard } \sigma} \right\|$ | $\left\| \dfrac{\hat{\theta} - \theta}{\text{corrected } \sigma} \right\|$ |
|---|---|---|---|---|
| $Z_\alpha$ | −0.1200 | -0.1177 | 1.0548 | 1.4207 |
| $Z_q$ | −0.0600 | -0.0611 | 0.7296 | 1.2435 |
| $Z_{\delta s}$ | −0.0496 | -0.0504 | 0.4106 | 0.4040 |
| $Z_o$ | 0.0000 | 0.0001 | 0.5446 | 0.5244 |
| $M_\alpha$ | −0.6600 | -0.6539 | 0.7539 | 0.9211 |
| $M_q$ | −0.1400 | -0.1447 | 0.7933 | 1.1264 |
| $M_{\delta s}$ | −1.3265 | -1.3405 | 1.0528 | 1.4058 |
| $M_o$ | 0.0000 | -0.0003 | 1.0208 | 1.4282 |
| $K_\alpha$ | 1.0000 | 0.9816 | 1.5406 | 2.5668 |
| $a_{z_o}$ | 0.0000 | -0.0007 | 0.9368 | 1.5153 |

**Table 2** LONGITUDINAL DYNAMIC MODEL PARAMETER ESTIMATES AND CRAMER-RAO BOUNDS - RUN 2 (white noise)

| Parameter | True Value, $\theta$ | Estimate, $\hat{\theta}$ | $\left\| \dfrac{\hat{\theta} - \theta}{\text{standard } \sigma} \right\|$ | $\left\| \dfrac{\hat{\theta} - \theta}{\text{corrected } \sigma} \right\|$ |
|---|---|---|---|---|
| $Z_\alpha$ | −0.1200 | -0.1209 | 0.4131 | 0.3967 |
| $Z_q$ | −0.0600 | -0.0585 | 1.0211 | 1.0842 |
| $Z_{\delta s}$ | −0.0496 | -0.0541 | 2.5239 | 2.0164 |
| $Z_o$ | 0.0000 | 0.0000 | 0.0664 | 0.1083 |
| $M_\alpha$ | −0.6600 | -0.6636 | 0.4567 | 0.4623 |
| $M_q$ | −0.1400 | -0.1500 | 1.6872 | 1.6888 |
| $M_{\delta s}$ | −1.3265 | -1.3275 | 0.0767 | 0.0677 |
| $M_o$ | 0.0000 | 0.0001 | 0.2690 | 0.3230 |
| $K_\alpha$ | 1.0000 | 1.0144 | 1.1990 | 1.0913 |
| $a_{z_o}$ | 0.0000 | -0.0001 | 0.1342 | 0.1777 |

**Table 3** LONGITUDINAL DYNAMIC MODEL PARAMETER ESTIMATES AND CRAMER-RAO BOUNDS - RUN 3 (white noise)

| Parameter | True Value, $\theta$ | Estimate, $\hat{\theta}$ | $\left\|\dfrac{\hat{\theta}-\theta}{\text{standard } \sigma}\right\|$ | $\left\|\dfrac{\hat{\theta}-\theta}{\text{corrected } \sigma}\right\|$ |
|---|---|---|---|---|
| $Z_\alpha$ | −0.1200 | -0.1221 | 0.9816 | 1.4478 |
| $Z_q$ | −0.0600 | -0.0585 | 1.0225 | 2.1056 |
| $Z_{\delta s}$ | −0.0496 | -0.0490 | 0.3159 | 0.4469 |
| $Z_o$ | 0.0000 | 0.0001 | 0.4658 | 0.9001 |
| $M_\alpha$ | −0.6600 | -0.6673 | 0.9080 | 0.9536 |
| $M_q$ | −0.1400 | -0.1361 | 0.6594 | 0.9567 |
| $M_{\delta s}$ | −1.3265 | -1.3218 | 0.3490 | 0.4327 |
| $M_o$ | 0.0000 | -0.0003 | 1.0256 | 1.2033 |
| $K_\alpha$ | 1.0000 | 0.9993 | 0.0597 | 0.0993 |
| $a_{z_o}$ | 0.0000 | -0.0006 | 0.8730 | 1.4775 |

**Table 4** LONGITUDINAL DYNAMIC MODEL PARAMETER ESTIMATES AND CRAMER-RAO BOUNDS - RUN 4 (white noise)

| Parameter | True Value, $\theta$ | Estimate, $\hat{\theta}$ | $\left\|\dfrac{\hat{\theta}-\theta}{\text{standard } \sigma}\right\|$ | $\left\|\dfrac{\hat{\theta}-\theta}{\text{corrected } \sigma}\right\|$ |
|---|---|---|---|---|
| $Z_\alpha$ | −0.1200 | -0.1202 | 0.0841 | 0.0959 |
| $Z_q$ | −0.0600 | -0.0585 | 1.0499 | 1.8280 |
| $Z_{\delta s}$ | −0.0496 | -0.0484 | 0.6696 | 0.6834 |
| $Z_o$ | 0.0000 | 0.0000 | 0.0428 | 0.0442 |
| $M_\alpha$ | −0.6600 | -0.6619 | 0.2438 | 0.2520 |
| $M_q$ | −0.1400 | -0.1356 | 0.7730 | 1.1375 |
| $M_{\delta s}$ | −1.3265 | -1.3294 | 0.2257 | 0.2718 |
| $M_o$ | 0.0000 | -0.0002 | 0.6695 | 0.7191 |
| $K_\alpha$ | 1.0000 | 0.9872 | 1.0725 | 1.4470 |
| $a_{z_o}$ | 0.0000 | -0.0002 | 0.3259 | 0.4406 |

**Table 5** LONGITUDINAL DYNAMIC MODEL PARAMETER ESTIMATES AND CRAMER-RAO BOUNDS - RUN 5 (white noise)

| Parameter | True Value, $\theta$ | Estimate, $\hat{\theta}$ | $\left\|\dfrac{\hat{\theta}-\theta}{\text{standard } \sigma}\right\|$ | $\left\|\dfrac{\hat{\theta}-\theta}{\text{corrected } \sigma}\right\|$ |
|---|---|---|---|---|
| $Z_\alpha$ | −0.1200 | -0.1227 | 1.2756 | 1.6603 |
| $Z_q$ | −0.0600 | -0.0592 | 0.5819 | 0.7766 |
| $Z_{\delta s}$ | −0.0496 | -0.0471 | 1.4643 | 1.6532 |
| $Z_o$ | 0.0000 | 0.0001 | 0.5712 | 0.8265 |
| $M_\alpha$ | −0.6600 | -0.6638 | 0.4640 | 0.6219 |
| $M_q$ | −0.1400 | -0.1410 | 0.1600 | 0.1766 |
| $M_{\delta s}$ | −1.3265 | -1.3114 | 1.1265 | 1.2809 |
| $M_o$ | 0.0000 | -0.0003 | 1.0805 | 1.5154 |
| $K_\alpha$ | 1.0000 | 1.0137 | 1.0843 | 1.4075 |
| $a_{z_o}$ | 0.0000 | -0.0010 | 1.3312 | 2.2710 |

**Table 6** LONGITUDINAL DYNAMIC MODEL PARAMETER ESTIMATES AND CRAMER-RAO BOUNDS - RUN 6 (white noise)

| Parameter | True Value, $\theta$ | Estimate, $\hat{\theta}$ | $\left\|\dfrac{\hat{\theta}-\theta}{\text{standard } \sigma}\right\|$ | $\left\|\dfrac{\hat{\theta}-\theta}{\text{corrected } \sigma}\right\|$ |
|---|---|---|---|---|
| $Z_\alpha$ | −0.1200 | -0.1221 | 0.9482 | 1.4726 |
| $Z_q$ | −0.0600 | -0.0607 | 0.4725 | 0.8838 |
| $Z_{\delta s}$ | −0.0496 | -0.0509 | 0.6952 | 0.8868 |
| $Z_o$ | 0.0000 | 0.0000 | 0.1016 | 0.2306 |
| $M_\alpha$ | −0.6600 | -0.6714 | 1.3503 | 1.7707 |
| $M_q$ | −0.1400 | -0.1421 | 0.3458 | 0.5127 |
| $M_{\delta s}$ | −1.3265 | -1.2985 | 2.0312 | 2.8107 |
| $M_o$ | 0.0000 | -0.0003 | 0.8904 | 1.3496 |
| $K_\alpha$ | 1.0000 | 1.0071 | 0.5587 | 0.9856 |
| $a_{z_o}$ | 0.0000 | 0.0004 | 0.5209 | 1.0113 |

23

**Table 7** LONGITUDINAL DYNAMIC MODEL PARAMETER ESTIMATES AND CRAMER-RAO BOUNDS - RUN 7 (white noise)

| Parameter | True Value, $\theta$ | Estimate, $\hat{\theta}$ | $\left\|\dfrac{\hat{\theta}-\theta}{\text{standard } \sigma}\right\|$ | $\left\|\dfrac{\hat{\theta}-\theta}{\text{corrected } \sigma}\right\|$ |
|---|---|---|---|---|
| $Z_\alpha$ | −0.1200 | -0.1230 | 1.3563 | 1.8503 |
| $Z_q$ | −0.0600 | -0.0594 | 0.3911 | 0.6524 |
| $Z_{\delta s}$ | −0.0496 | -0.0475 | 1.1131 | 1.4936 |
| $Z_o$ | 0.0000 | -0.0002 | 0.9742 | 1.4870 |
| $M_\alpha$ | −0.6600 | -0.6599 | 0.0086 | 0.0086 |
| $M_q$ | −0.1400 | -0.1434 | 0.5610 | 0.7487 |
| $M_{\delta s}$ | −1.3265 | -1.3175 | 0.6618 | 0.7779 |
| $M_o$ | 0.0000 | -0.0005 | 1.7136 | 1.7471 |
| $K_\alpha$ | 1.0000 | 1.0051 | 0.4151 | 0.4524 |
| $a_{z_o}$ | 0.0000 | -0.0008 | 1.0277 | 1.5639 |

**Table 8** LONGITUDINAL DYNAMIC MODEL PARAMETER ESTIMATES AND CRAMER-RAO BOUNDS - RUN 8 (white noise)

| Parameter | True Value, $\theta$ | Estimate, $\hat{\theta}$ | $\left\|\dfrac{\hat{\theta}-\theta}{\text{standard } \sigma}\right\|$ | $\left\|\dfrac{\hat{\theta}-\theta}{\text{corrected } \sigma}\right\|$ |
|---|---|---|---|---|
| $Z_\alpha$ | −0.1200 | -0.1189 | 0.5204 | 0.6378 |
| $Z_q$ | −0.0600 | -0.0608 | 0.5574 | 0.7960 |
| $Z_{\delta s}$ | −0.0496 | -0.0534 | 2.0626 | 2.1984 |
| $Z_o$ | 0.0000 | 0.0001 | 0.2962 | 0.6148 |
| $M_\alpha$ | −0.6600 | -0.6591 | 0.1022 | 0.1091 |
| $M_q$ | −0.1400 | -0.1488 | 1.4299 | 1.5541 |
| $M_{\delta s}$ | −1.3265 | -1.3376 | 0.8098 | 0.9708 |
| $M_o$ | 0.0000 | -0.0002 | 0.7846 | 1.2381 |
| $K_\alpha$ | 1.0000 | 0.9856 | 1.1581 | 1.3866 |
| $a_{z_o}$ | 0.0000 | 0.0001 | 0.1900 | 0.3346 |

**Table 9** LONGITUDINAL DYNAMIC MODEL PARAMETER ESTIMATES AND
CRAMER-RAO BOUNDS - RUN 9 (white noise)

| Parameter | True Value, $\theta$ | Estimate, $\hat{\theta}$ | $\left\|\dfrac{\hat{\theta} - \theta}{\text{standard } \sigma}\right\|$ | $\left\|\dfrac{\hat{\theta} - \theta}{\text{corrected } \sigma}\right\|$ |
|---|---|---|---|---|
| $Z_\alpha$ | −0.1200 | -0.1176 | 1.1423 | 1.5923 |
| $Z_q$ | −0.0600 | -0.0618 | 1.2403 | 2.3168 |
| $Z_{\delta s}$ | −0.0496 | -0.0491 | 0.2888 | 0.3086 |
| $Z_o$ | 0.0000 | -0.0001 | 0.2937 | 0.6062 |
| $M_\alpha$ | −0.6600 | -0.6697 | 1.2030 | 1.2607 |
| $M_q$ | −0.1400 | -0.1377 | 0.3846 | 0.6424 |
| $M_{\delta s}$ | −1.3265 | -1.3222 | 0.3165 | 0.3578 |
| $M_o$ | 0.0000 | -0.0002 | 0.7802 | 1.0720 |
| $K_\alpha$ | 1.0000 | 0.9875 | 1.0244 | 1.4360 |
| $a_{z_o}$ | 0.0000 | -0.0002 | 0.3095 | 0.5527 |

**Table 10** LONGITUDINAL DYNAMIC MODEL PARAMETER ESTIMATES AND
CRAMER-RAO BOUNDS - RUN 10 (white noise)

| Parameter | True Value, $\theta$ | Estimate, $\hat{\theta}$ | $\left\|\dfrac{\hat{\theta} - \theta}{\text{standard } \sigma}\right\|$ | $\left\|\dfrac{\hat{\theta} - \theta}{\text{corrected } \sigma}\right\|$ |
|---|---|---|---|---|
| $Z_\alpha$ | −0.1200 | -0.1196 | 0.1822 | 0.2446 |
| $Z_q$ | −0.0600 | -0.0616 | 1.0827 | 1.6376 |
| $Z_{\delta s}$ | −0.0496 | -0.0516 | 1.0752 | 1.4153 |
| $Z_o$ | 0.0000 | 0.0000 | 0.1337 | 0.3304 |
| $M_\alpha$ | −0.6600 | -0.6582 | 0.2270 | 0.3590 |
| $M_q$ | −0.1400 | -0.1324 | 1.2841 | 1.6340 |
| $M_{\delta s}$ | −1.3265 | -1.3196 | 0.5162 | 0.6758 |
| $M_o$ | 0.0000 | 0.0001 | 0.3587 | 0.7559 |
| $K_\alpha$ | 1.0000 | 1.0001 | 0.0083 | 0.0098 |
| $a_{z_o}$ | 0.0000 | 0.0006 | 0.7700 | 1.5711 |

**Table 11** LONGITUDINAL DYNAMIC MODEL PARAMETER ESTIMATES AND
CRAMER-RAO BOUNDS - RUN 11 (band limited noise)

| Parameter | True Value, $\theta$ | Estimate, $\hat{\theta}$ | $\left\|\dfrac{\hat{\theta}-\theta}{\text{standard } \sigma}\right\|$ | $\left\|\dfrac{\hat{\theta}-\theta}{\text{corrected } \sigma}\right\|$ |
|---|---|---|---|---|
| $Z_\alpha$ | −0.1200 | -0.1149 | 2.8625 | 0.5850 |
| $Z_q$ | −0.0600 | -0.0619 | 1.4836 | 0.3219 |
| $Z_{\delta s}$ | −0.0496 | -0.0682 | 12.367 | 1.5388 |
| $Z_o$ | 0.0000 | -0.0012 | 5.1209 | 1.5395 |
| $M_\alpha$ | −0.6600 | -0.7419 | 12.371 | 2.3583 |
| $M_q$ | −0.1400 | -0.0890 | 11.658 | 2.6873 |
| $M_{\delta s}$ | −1.3265 | -1.2245 | 8.6593 | 1.6371 |
| $M_o$ | 0.0000 | -0.0029 | 10.913 | 2.2833 |
| $K_\alpha$ | 1.0000 | 0.8941 | 10.887 | 2.4662 |
| $a_{z_o}$ | 0.0000 | 0.0022 | 3.4780 | 0.7790 |

**Table 12** LONGITUDINAL DYNAMIC MODEL PARAMETER ESTIMATES AND
CRAMER-RAO BOUNDS - RUN 12 (band limited noise)

| Parameter | True Value, $\theta$ | Estimate, $\hat{\theta}$ | $\left\|\dfrac{\hat{\theta}-\theta}{\text{standard } \sigma}\right\|$ | $\left\|\dfrac{\hat{\theta}-\theta}{\text{corrected } \sigma}\right\|$ |
|---|---|---|---|---|
| $Z_\alpha$ | −0.1200 | -0.0994 | 13.290 | 2.6056 |
| $Z_q$ | −0.0600 | -0.0707 | 9.8702 | 2.0558 |
| $Z_{\delta s}$ | −0.0496 | -0.0544 | 3.7855 | 0.5116 |
| $Z_o$ | 0.0000 | 0.0006 | 2.6205 | 0.5521 |
| $M_\alpha$ | −0.6600 | -0.6357 | 3.1622 | 0.5429 |
| $M_q$ | −0.1400 | -0.2010 | 10.054 | 1.8170 |
| $M_{\delta s}$ | −1.3265 | -1.4017 | 5.7487 | 1.0385 |
| $M_o$ | 0.0000 | -0.0013 | 4.4388 | 0.9535 |
| $K_\alpha$ | 1.0000 | 0.9231 | 6.7654 | 1.4972 |
| $a_{z_o}$ | 0.0000 | 0.0025 | 4.3671 | 1.0023 |

**Table 13** LONGITUDINAL DYNAMIC MODEL PARAMETER ESTIMATES AND CRAMER-RAO BOUNDS - RUN 13 (band limited noise)

| Parameter | True Value, $\theta$ | Estimate, $\hat{\theta}$ | $\left\|\dfrac{\hat{\theta}-\theta}{\text{standard }\sigma}\right\|$ | $\left\|\dfrac{\hat{\theta}-\theta}{\text{corrected }\sigma}\right\|$ |
|---|---|---|---|---|
| $Z_\alpha$ | −0.1200 | -0.1099 | 5.1625 | 0.9119 |
| $Z_q$ | −0.0600 | -0.0621 | 1.4541 | 0.2987 |
| $Z_{\delta s}$ | −0.0496 | -0.0699 | 11.311 | 1.8446 |
| $Z_o$ | 0.0000 | 0.0033 | 16.282 | 1.9158 |
| $M_\alpha$ | −0.6600 | -0.5983 | 8.099 | 1.3766 |
| $M_q$ | −0.1400 | -0.1512 | 1.9002 | 0.3340 |
| $M_{\delta s}$ | −1.3265 | -1.3681 | 3.6237 | 0.5943 |
| $M_o$ | 0.0000 | 0.0003 | 1.2479 | 0.2248 |
| $K_\alpha$ | 1.0000 | 0.8803 | 12.575 | 2.4115 |
| $a_{z_o}$ | 0.0000 | 0.0008 | 1.0877 | 0.2456 |

**Table 14** LONGITUDINAL DYNAMIC MODEL PARAMETER ESTIMATES AND CRAMER-RAO BOUNDS - RUN 14 (band limited noise)

| Parameter | True Value, $\theta$ | Estimate, $\hat{\theta}$ | $\left\|\dfrac{\hat{\theta}-\theta}{\text{standard }\sigma}\right\|$ | $\left\|\dfrac{\hat{\theta}-\theta}{\text{corrected }\sigma}\right\|$ |
|---|---|---|---|---|
| $Z_\alpha$ | −0.1200 | -0.1081 | 8.3870 | 1.3979 |
| $Z_q$ | −0.0600 | -0.0731 | 12.996 | 2.3744 |
| $Z_{\delta s}$ | −0.0496 | -0.0615 | 9.1655 | 1.2917 |
| $Z_o$ | 0.0000 | 0.0000 | 0.1282 | 0.0286 |
| $M_\alpha$ | −0.6600 | -0.5681 | 17.640 | 2.6978 |
| $M_q$ | −0.1400 | -0.1354 | 0.9946 | 0.1601 |
| $M_{\delta s}$ | −1.3265 | -1.5225 | 19.407 | 2.6978 |
| $M_o$ | 0.0000 | 0.0024 | 12.510 | 2.0434 |
| $K_\alpha$ | 1.0000 | 0.9276 | 8.2949 | 1.3658 |
| $a_{z_o}$ | 0.0000 | -0.0050 | 9.2577 | 1.8631 |

**Table 15** LONGITUDINAL DYNAMIC MODEL PARAMETER ESTIMATES AND CRAMER-RAO BOUNDS - RUN 15 (band limited noise)

| Parameter | True Value, $\theta$ | Estimate, $\hat{\theta}$ | $\left\|\dfrac{\hat{\theta}-\theta}{\text{standard }\sigma}\right\|$ | $\left\|\dfrac{\hat{\theta}-\theta}{\text{corrected }\sigma}\right\|$ |
|---|---|---|---|---|
| $Z_\alpha$ | −0.1200 | -0.1045 | 8.3263 | 1.6232 |
| $Z_q$ | −0.0600 | -0.0679 | 5.7664 | 1.4616 |
| $Z_{\delta s}$ | −0.0496 | -0.0598 | 5.8118 | 1.0155 |
| $Z_o$ | 0.0000 | 0.0014 | 6.5776 | 0.7742 |
| $M_\alpha$ | −0.6600 | -0.5980 | 8.3445 | 1.3884 |
| $M_q$ | −0.1400 | -0.1786 | 6.7034 | 1.1026 |
| $M_{\delta s}$ | −1.3265 | -1.4396 | 9.5540 | 1.5099 |
| $M_o$ | 0.0000 | -0.0014 | 5.5733 | 0.9312 |
| $K_\alpha$ | 1.0000 | 0.8851 | 11.832 | 2.3743 |
| $a_{z_o}$ | 0.0000 | -0.0039 | 5.3693 | 1.1936 |

**Table 16** LONGITUDINAL DYNAMIC MODEL PARAMETER ESTIMATES AND CRAMER-RAO BOUNDS - RUN 16 (band limited noise)

| Parameter | True Value, $\theta$ | Estimate, $\hat{\theta}$ | $\left\|\dfrac{\hat{\theta}-\theta}{\text{standard }\sigma}\right\|$ | $\left\|\dfrac{\hat{\theta}-\theta}{\text{corrected }\sigma}\right\|$ |
|---|---|---|---|---|
| $Z_\alpha$ | −0.1200 | -0.1124 | 4.6543 | 0.9482 |
| $Z_q$ | −0.0600 | -0.0563 | 3.3345 | 0.7702 |
| $Z_{\delta s}$ | −0.0496 | -0.0610 | 7.9378 | 1.0951 |
| $Z_o$ | 0.0000 | 0.0017 | 7.5169 | 2.6730 |
| $M_\alpha$ | −0.6600 | -0.6657 | 0.8029 | 0.1566 |
| $M_q$ | −0.1400 | -0.1300 | 1.9607 | 0.4864 |
| $M_{\delta s}$ | −1.3265 | -1.3777 | 4.2624 | 0.8354 |
| $M_o$ | 0.0000 | -0.0032 | 11.224 | 2.3899 |
| $K_\alpha$ | 1.0000 | 0.8907 | 10.786 | 2.7068 |
| $a_{z_o}$ | 0.0000 | 0.0010 | 1.5965 | 0.3650 |

28

**Table 17** LONGITUDINAL DYNAMIC MODEL PARAMETER ESTIMATES AND CRAMER-RAO BOUNDS - RUN 17 (band limited noise)

| Parameter | True Value, $\theta$ | Estimate, $\hat{\theta}$ | $\left\| \dfrac{\hat{\theta} - \theta}{\text{standard } \sigma} \right\|$ | $\left\| \dfrac{\hat{\theta} - \theta}{\text{corrected } \sigma} \right\|$ |
|---|---|---|---|---|
| $Z_\alpha$ | −0.1200 | -0.1330 | 6.1532 | 1.2228 |
| $Z_q$ | −0.0600 | -0.0559 | 2.8302 | 0.6600 |
| $Z_{\delta s}$ | −0.0496 | -0.0446 | 2.8864 | 0.4214 |
| $Z_o$ | 0.0000 | -0.0008 | 3.1786 | 0.7223 |
| $M_\alpha$ | −0.6600 | -0.6674 | 0.9175 | 0.1392 |
| $M_q$ | −0.1400 | -0.1669 | 4.3509 | 0.6964 |
| $M_{\delta s}$ | −1.3265 | -1.3144 | 0.9017 | 0.1410 |
| $M_o$ | 0.0000 | 0.0006 | 2.1354 | 0.4174 |
| $K_\alpha$ | 1.0000 | 0.9871 | 1.0957 | 0.2132 |
| $a_{z_o}$ | 0.0000 | -0.0063 | 8.9763 | 2.1863 |

**Table 18** LONGITUDINAL DYNAMIC MODEL PARAMETER ESTIMATES AND CRAMER-RAO BOUNDS - RUN 18 (band limited noise)

| Parameter | True Value, $\theta$ | Estimate, $\hat{\theta}$ | $\left\| \dfrac{\hat{\theta} - \theta}{\text{standard } \sigma} \right\|$ | $\left\| \dfrac{\hat{\theta} - \theta}{\text{corrected } \sigma} \right\|$ |
|---|---|---|---|---|
| $Z_\alpha$ | −0.1200 | -0.1258 | 3.3745 | 0.7023 |
| $Z_q$ | −0.0600 | -0.0616 | 1.4015 | 0.3568 |
| $Z_{\delta s}$ | −0.0496 | -0.0394 | 7.2608 | 1.3276 |
| $Z_o$ | 0.0000 | -0.0004 | 1.8180 | 0.3257 |
| $M_\alpha$ | −0.6600 | -0.7327 | 9.6633 | 1.4463 |
| $M_q$ | −0.1400 | -0.1669 | 5.2334 | 1.0887 |
| $M_{\delta s}$ | −1.3265 | -1.2966 | 2.4478 | 0.4103 |
| $M_o$ | 0.0000 | -0.0027 | 9.9423 | 1.6606 |
| $K_\alpha$ | 1.0000 | 1.0656 | 5.7806 | 1.1744 |
| $a_{z_o}$ | 0.0000 | 0.0009 | 1.5384 | 0.3534 |

**Table 19** LONGITUDINAL DYNAMIC MODEL PARAMETER ESTIMATES AND CRAMER-RAO BOUNDS - RUN 19 (band limited noise)

| Parameter | True Value, $\theta$ | Estimate, $\hat{\theta}$ | $\left\|\dfrac{\hat{\theta}-\theta}{\text{standard }\sigma}\right\|$ | $\left\|\dfrac{\hat{\theta}-\theta}{\text{corrected }\sigma}\right\|$ |
|---|---|---|---|---|
| $Z_\alpha$ | −0.1200 | -0.1087 | 6.2247 | 1.0573 |
| $Z_q$ | −0.0600 | -0.0721 | 9.2315 | 1.5896 |
| $Z_{\delta s}$ | −0.0496 | -0.0751 | 16.660 | 2.1714 |
| $Z_o$ | 0.0000 | -0.0007 | 3.0161 | 0.9104 |
| $M_\alpha$ | −0.6600 | -0.6194 | 5.2636 | 0.7920 |
| $M_q$ | −0.1400 | -0.2087 | 10.602 | 2.0165 |
| $M_{\delta s}$ | −1.3265 | -1.4105 | 6.1350 | 0.9313 |
| $M_o$ | 0.0000 | 0.0009 | 3.5568 | 0.6639 |
| $K_\alpha$ | 1.0000 | 0.9515 | 4.3324 | 0.7987 |
| $a_{z_o}$ | 0.0000 | 0.0016 | 2.5690 | 0.5834 |

**Table 20** LONGITUDINAL DYNAMIC MODEL PARAMETER ESTIMATES AND CRAMER-RAO BOUNDS - RUN 20 (band limited noise)

| Parameter | True Value, $\theta$ | Estimate, $\hat{\theta}$ | $\left\|\dfrac{\hat{\theta}-\theta}{\text{standard }\sigma}\right\|$ | $\left\|\dfrac{\hat{\theta}-\theta}{\text{corrected }\sigma}\right\|$ |
|---|---|---|---|---|
| $Z_\alpha$ | −0.1200 | -0.1383 | 8.2762 | 1.6074 |
| $Z_q$ | −0.0600 | -0.0738 | 8.8645 | 1.6306 |
| $Z_{\delta s}$ | −0.0496 | -0.0535 | 2.2699 | 0.3648 |
| $Z_o$ | 0.0000 | -0.0010 | 4.7563 | 0.9479 |
| $M_\alpha$ | −0.6600 | -0.6931 | 4.7258 | 0.9052 |
| $M_q$ | −0.1400 | -0.1183 | 4.2280 | 0.8128 |
| $M_{\delta s}$ | −1.3265 | -1.1958 | 11.693 | 2.5125 |
| $M_o$ | 0.0000 | 0.0016 | 7.6997 | 1.8215 |
| $K_\alpha$ | 1.0000 | 1.1679 | 13.186 | 3.2653 |
| $a_{z_o}$ | 0.0000 | 0.0050 | 7.6176 | 1.9777 |

**Table 21** LONGITUDINAL DYNAMIC MODEL PARAMETER ESTIMATES AND
CRAMER-RAO BOUNDS - RUN 21  (colored noise)

| Parameter | True Value, $\theta$ | Estimate, $\hat{\theta}$ | $\left\|\dfrac{\hat{\theta}-\theta}{\text{standard } \sigma}\right\|$ | $\left\|\dfrac{\hat{\theta}-\theta}{\text{corrected } \sigma}\right\|$ |
|---|---|---|---|---|
| $Z_\alpha$ | −0.1200 | -0.1061 | 7.5168 | 1.3607 |
| $Z_q$ | −0.0600 | -0.0533 | 4.9643 | 1.1594 |
| $Z_{\delta s}$ | −0.0496 | -0.0545 | 2.6371 | 0.4190 |
| $Z_o$ | 0.0000 | 0.0011 | 4.7742 | 1.4312 |
| $M_\alpha$ | −0.6600 | -0.6146 | 5.6133 | 0.9139 |
| $M_q$ | −0.1400 | -0.2056 | 10.611 | 1.8809 |
| $M_{\delta s}$ | −1.3265 | -1.5247 | 14.548 | 2.2400 |
| $M_o$ | 0.0000 | -0.0003 | 1.1757 | 0.2369 |
| $K_\alpha$ | 1.0000 | 0.8501 | 15.686 | 3.2294 |
| $a_{z_o}$ | 0.0000 | 0.0051 | 6.8756 | 1.6655 |

**Table 22** LONGITUDINAL DYNAMIC MODEL PARAMETER ESTIMATES AND
CRAMER-RAO BOUNDS - RUN 22  (colored noise)

| Parameter | True Value, $\theta$ | Estimate, $\hat{\theta}$ | $\left\|\dfrac{\hat{\theta}-\theta}{\text{standard } \sigma}\right\|$ | $\left\|\dfrac{\hat{\theta}-\theta}{\text{corrected } \sigma}\right\|$ |
|---|---|---|---|---|
| $Z_\alpha$ | −0.1200 | -0.0980 | 12.151 | 2.4711 |
| $Z_q$ | −0.0600 | -0.0596 | 0.3084 | 0.0843 |
| $Z_{\delta s}$ | −0.0496 | -0.0727 | 13.159 | 2.3480 |
| $Z_o$ | 0.0000 | 0.0025 | 11.567 | 2.1292 |
| $M_\alpha$ | −0.6600 | -0.6460 | 1.9121 | 0.2917 |
| $M_q$ | −0.1400 | -0.1039 | 7.1132 | 1.2110 |
| $M_{\delta s}$ | −1.3265 | -1.3936 | 5.6630 | 0.9275 |
| $M_o$ | 0.0000 | -0.0001 | 0.3830 | 0.0599 |
| $K_\alpha$ | 1.0000 | 0.8992 | 9.6421 | 1.7422 |
| $a_{z_o}$ | 0.0000 | 0.0031 | 4.4546 | 1.0164 |

**Table 23** LONGITUDINAL DYNAMIC MODEL PARAMETER ESTIMATES AND CRAMER-RAO BOUNDS - RUN 23 (colored noise)

| Parameter | True Value, $\theta$ | Estimate, $\hat{\theta}$ | $\left\|\dfrac{\hat{\theta}-\theta}{\text{standard } \sigma}\right\|$ | $\left\|\dfrac{\hat{\theta}-\theta}{\text{corrected } \sigma}\right\|$ |
|---|---|---|---|---|
| $Z_\alpha$ | −0.1200 | -0.1392 | 9.4275 | 1.8622 |
| $Z_q$ | −0.0600 | -0.0618 | 1.3040 | 0.3227 |
| $Z_{\delta s}$ | −0.0496 | -0.0379 | 7.2643 | 1.1618 |
| $Z_o$ | 0.0000 | 0.0016 | 8.0830 | 1.0965 |
| $M_\alpha$ | −0.6600 | -0.8052 | 19.129 | 2.9224 |
| $M_q$ | −0.1400 | -0.0535 | 20.405 | 3.1831 |
| $M_{\delta s}$ | −1.3265 | -1.1171 | 18.589 | 2.9508 |
| $M_o$ | 0.0000 | -0.0036 | 13.580 | 2.0105 |
| $K_\alpha$ | 1.0000 | 1.1461 | 12.255 | 1.8967 |
| $a_{z_o}$ | 0.0000 | -0.0114 | 16.743 | 3.4106 |

**Table 24** LONGITUDINAL DYNAMIC MODEL PARAMETER ESTIMATES AND CRAMER-RAO BOUNDS - RUN 24 (colored noise)

| Parameter | True Value, $\theta$ | Estimate, $\hat{\theta}$ | $\left\|\dfrac{\hat{\theta}-\theta}{\text{standard } \sigma}\right\|$ | $\left\|\dfrac{\hat{\theta}-\theta}{\text{corrected } \sigma}\right\|$ |
|---|---|---|---|---|
| $Z_\alpha$ | −0.1200 | -0.1027 | 9.8009 | 2.0916 |
| $Z_q$ | −0.0600 | -0.0704 | 8.1676 | 2.1834 |
| $Z_{\delta s}$ | −0.0496 | -0.0603 | 6.5715 | 1.2755 |
| $Z_o$ | 0.0000 | 0.0019 | 8.7375 | 2.8303 |
| $M_\alpha$ | −0.6600 | -0.6089 | 6.6303 | 1.1690 |
| $M_q$ | −0.1400 | -0.1711 | 5.1944 | 0.9892 |
| $M_{\delta s}$ | −1.3265 | -1.4595 | 10.420 | 1.7979 |
| $M_o$ | 0.0000 | 0.0025 | 10.118 | 1.9189 |
| $K_\alpha$ | 1.0000 | 0.9955 | 0.3821 | 0.0893 |
| $a_{z_o}$ | 0.0000 | 0.0066 | 10.434 | 2.7255 |

32

**Table 25** LONGITUDINAL DYNAMIC MODEL PARAMETER ESTIMATES AND CRAMER-RAO BOUNDS - RUN 25  (colored noise)

| Parameter | True Value, $\theta$ | Estimate, $\hat{\theta}$ | $\left\| \dfrac{\hat{\theta}-\theta}{\text{standard } \sigma} \right\|$ | $\left\| \dfrac{\hat{\theta}-\theta}{\text{corrected } \sigma} \right\|$ |
|---|---|---|---|---|
| $Z_\alpha$ | −0.1200 | -0.1257 | 3.0188 | 0.5376 |
| $Z_q$ | −0.0600 | -0.0580 | 1.5276 | 0.2589 |
| $Z_{\delta s}$ | −0.0496 | -0.0407 | 5.3341 | 0.7403 |
| $Z_o$ | 0.0000 | -0.0017 | 7.3544 | 1.5254 |
| $M_\alpha$ | −0.6600 | -0.5431 | 16.323 | 2.9242 |
| $M_q$ | −0.1400 | -0.2109 | 10.844 | 1.7878 |
| $M_{\delta s}$ | −1.3265 | -1.5004 | 13.443 | 2.2870 |
| $M_o$ | 0.0000 | 0.0028 | 12.062 | 2.2904 |
| $K_\alpha$ | 1.0000 | 0.9085 | 8.8839 | 1.5744 |
| $a_{z_o}$ | 0.0000 | -0.0061 | 8.8680 | 2.0119 |

**Table 26** LONGITUDINAL DYNAMIC MODEL PARAMETER ESTIMATES AND CRAMER-RAO BOUNDS - RUN 26  (colored noise)

| Parameter | True Value, $\theta$ | Estimate, $\hat{\theta}$ | $\left\| \dfrac{\hat{\theta}-\theta}{\text{standard } \sigma} \right\|$ | $\left\| \dfrac{\hat{\theta}-\theta}{\text{corrected } \sigma} \right\|$ |
|---|---|---|---|---|
| $Z_\alpha$ | −0.1200 | -0.1403 | 10.344 | 2.1157 |
| $Z_q$ | −0.0600 | -0.0491 | 8.6461 | 2.2289 |
| $Z_{\delta s}$ | −0.0496 | -0.0293 | 13.587 | 3.2656 |
| $Z_o$ | 0.0000 | -0.0027 | 10.554 | 2.8641 |
| $M_\alpha$ | −0.6600 | -0.6383 | 3.0224 | 0.4923 |
| $M_q$ | −0.1400 | -0.1871 | 7.5879 | 1.2408 |
| $M_{\delta s}$ | −1.3265 | -1.3930 | 4.7080 | 0.7781 |
| $M_o$ | 0.0000 | 0.0023 | 9.1923 | 1.5604 |
| $K_\alpha$ | 1.0000 | 1.0088 | 0.7208 | 0.1160 |
| $a_{z_o}$ | 0.0000 | -0.0060 | 9.4544 | 2.1602 |

**Table 27** LONGITUDINAL DYNAMIC MODEL PARAMETER ESTIMATES AND CRAMER-RAO BOUNDS - RUN 27  (colored noise)

| Parameter | True Value, $\theta$ | Estimate, $\hat{\theta}$ | $\dfrac{\|\hat{\theta} - \theta\|}{\text{standard } \sigma}$ | $\dfrac{\|\hat{\theta} - \theta\|}{\text{corrected } \sigma}$ |
|---|---|---|---|---|
| $Z_\alpha$ | −0.1200 | -0.1282 | 3.8259 | 0.7433 |
| $Z_q$ | −0.0600 | -0.0637 | 2.4450 | 0.4965 |
| $Z_{\delta s}$ | −0.0496 | -0.0569 | 4.3716 | 0.6075 |
| $Z_o$ | 0.0000 | -0.0021 | 8.9336 | 2.8628 |
| $M_\alpha$ | −0.6600 | -0.5912 | 8.7992 | 1.5334 |
| $M_q$ | −0.1400 | -0.2033 | 9.2512 | 1.7920 |
| $M_{\delta s}$ | −1.3265 | -1.3229 | 0.2754 | 0.0477 |
| $M_o$ | 0.0000 | 0.0005 | 2.1958 | 0.4992 |
| $K_\alpha$ | 1.0000 | 1.0787 | 6.0239 | 1.1390 |
| $a_{z_o}$ | 0.0000 | -0.0062 | 8.7125 | 2.1701 |

**Table 28** LONGITUDINAL DYNAMIC MODEL PARAMETER ESTIMATES AND CRAMER-RAO BOUNDS - RUN 28  (colored noise)

| Parameter | True Value, $\theta$ | Estimate, $\hat{\theta}$ | $\dfrac{\|\hat{\theta} - \theta\|}{\text{standard } \sigma}$ | $\dfrac{\|\hat{\theta} - \theta\|}{\text{corrected } \sigma}$ |
|---|---|---|---|---|
| $Z_\alpha$ | −0.1200 | -0.1018 | 9.7989 | 1.8491 |
| $Z_q$ | −0.0600 | -0.0602 | 0.1275 | 0.0231 |
| $Z_{\delta s}$ | −0.0496 | -0.0709 | 13.386 | 1.9596 |
| $Z_o$ | 0.0000 | 0.0010 | 3.8657 | 1.4456 |
| $M_\alpha$ | −0.6600 | -0.6244 | 4.7377 | 0.8179 |
| $M_q$ | −0.1400 | -0.1187 | 3.5376 | 0.7562 |
| $M_{\delta s}$ | −1.3265 | -1.3361 | 0.7291 | 0.1450 |
| $M_o$ | 0.0000 | -0.0017 | 5.9438 | 1.4466 |
| $K_\alpha$ | 1.0000 | 0.8465 | 13.959 | 3.0485 |
| $a_{z_o}$ | 0.0000 | -0.0005 | 0.7315 | 0.1856 |

**Table 29** LONGITUDINAL DYNAMIC MODEL PARAMETER ESTIMATES AND CRAMER-RAO BOUNDS - RUN 29  (colored noise)

| Parameter | True Value, $\theta$ | Estimate, $\hat{\theta}$ | $\dfrac{\|\hat{\theta} - \theta\|}{\text{standard } \sigma}$ | $\dfrac{\|\hat{\theta} - \theta\|}{\text{corrected } \sigma}$ |
|---|---|---|---|---|
| $Z_\alpha$ | −0.1200 | -0.1053 | 7.9948 | 1.1955 |
| $Z_q$ | −0.0600 | -0.0527 | 5.4278 | 1.5089 |
| $Z_{\delta s}$ | −0.0496 | -0.0594 | 5.4603 | 0.9909 |
| $Z_o$ | 0.0000 | 0.0022 | 10.157 | 1.7000 |
| $M_\alpha$ | −0.6600 | -0.6366 | 3.5389 | 0.6381 |
| $M_q$ | −0.1400 | -0.1020 | 7.6247 | 1.4104 |
| $M_{\delta s}$ | −1.3265 | -1.3994 | 6.0895 | 1.1411 |
| $M_o$ | 0.0000 | 0.0015 | 6.6273 | 1.2007 |
| $K_\alpha$ | 1.0000 | 0.9739 | 2.5720 | 0.4449 |
| $a_{z_o}$ | 0.0000 | 0.0035 | 5.1899 | 1.0830 |

**Table 30** LONGITUDINAL DYNAMIC MODEL PARAMETER ESTIMATES AND CRAMER-RAO BOUNDS - RUN 30  (colored noise)

| Parameter | True Value, $\theta$ | Estimate, $\hat{\theta}$ | $\dfrac{\|\hat{\theta} - \theta\|}{\text{standard } \sigma}$ | $\dfrac{\|\hat{\theta} - \theta\|}{\text{corrected } \sigma}$ |
|---|---|---|---|---|
| $Z_\alpha$ | −0.1200 | -0.1303 | 4.8615 | 0.8891 |
| $Z_q$ | −0.0600 | -0.0619 | 1.2497 | 0.3016 |
| $Z_{\delta s}$ | −0.0496 | -0.0602 | 6.0041 | 0.9943 |
| $Z_o$ | 0.0000 | -0.0012 | 5.3350 | 1.0467 |
| $M_\alpha$ | −0.6600 | -0.7208 | 8.0705 | 1.2027 |
| $M_q$ | −0.1400 | -0.1472 | 1.3693 | 0.2678 |
| $M_{\delta s}$ | −1.3265 | -1.2376 | 7.3530 | 1.2539 |
| $M_o$ | 0.0000 | -0.0051 | 18.109 | 2.6469 |
| $K_\alpha$ | 1.0000 | 0.9600 | 3.8148 | 0.7254 |
| $a_{z_o}$ | 0.0000 | -0.0026 | 3.2722 | 0.6512 |

35
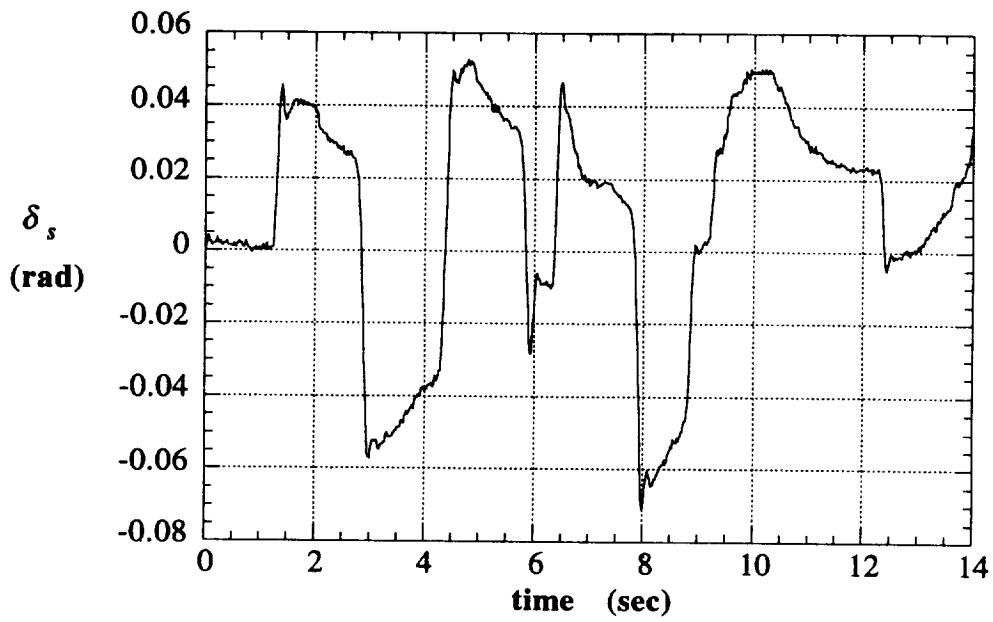
**Figure 1** Stabilator input
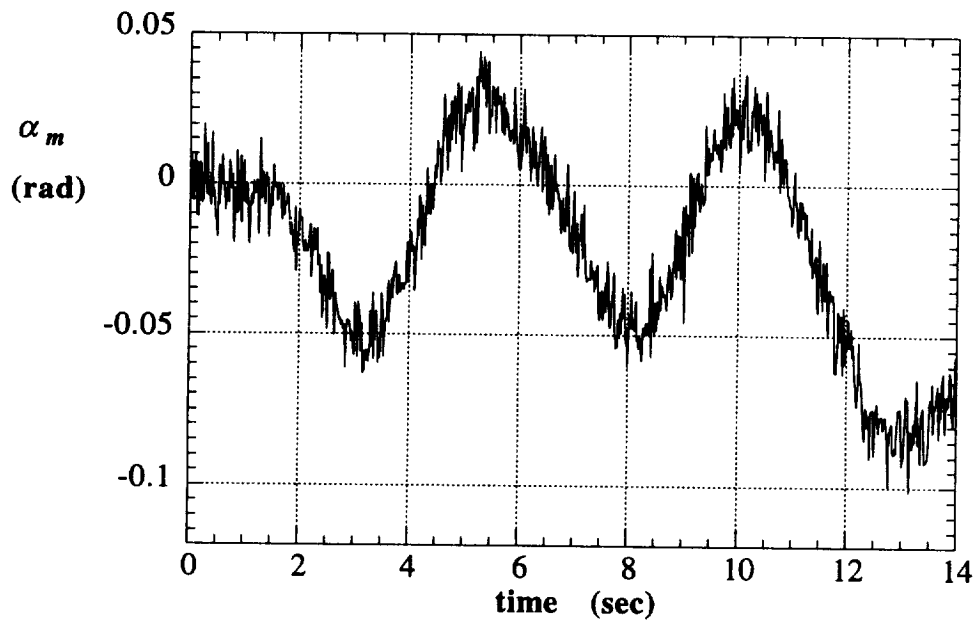


**Figure 2(a)** Simulated angle of attack with white measurement noise
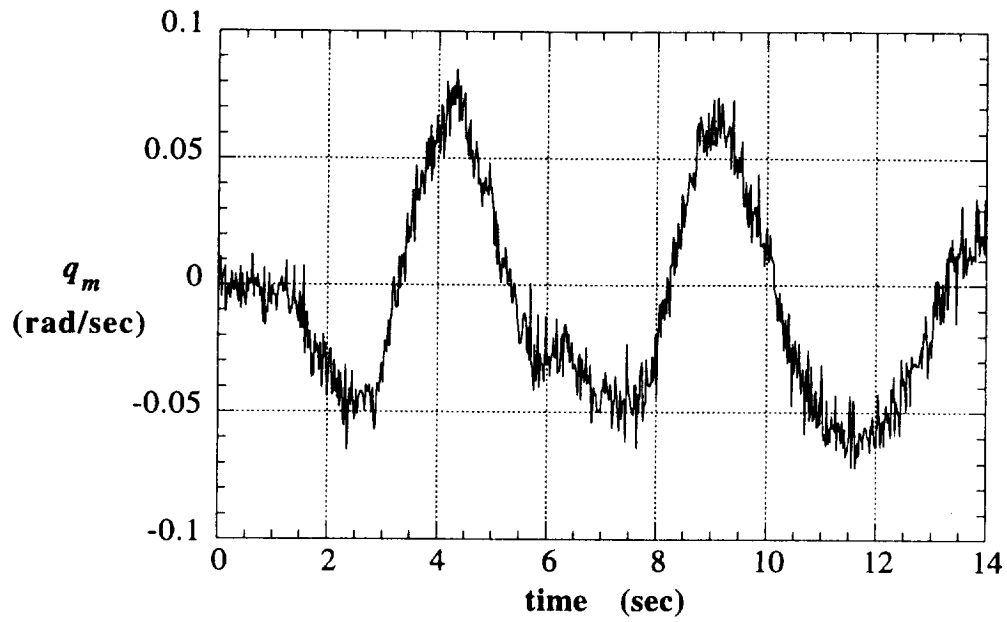
**Figure 2(b)** Simulated pitch rate with white measurement noise
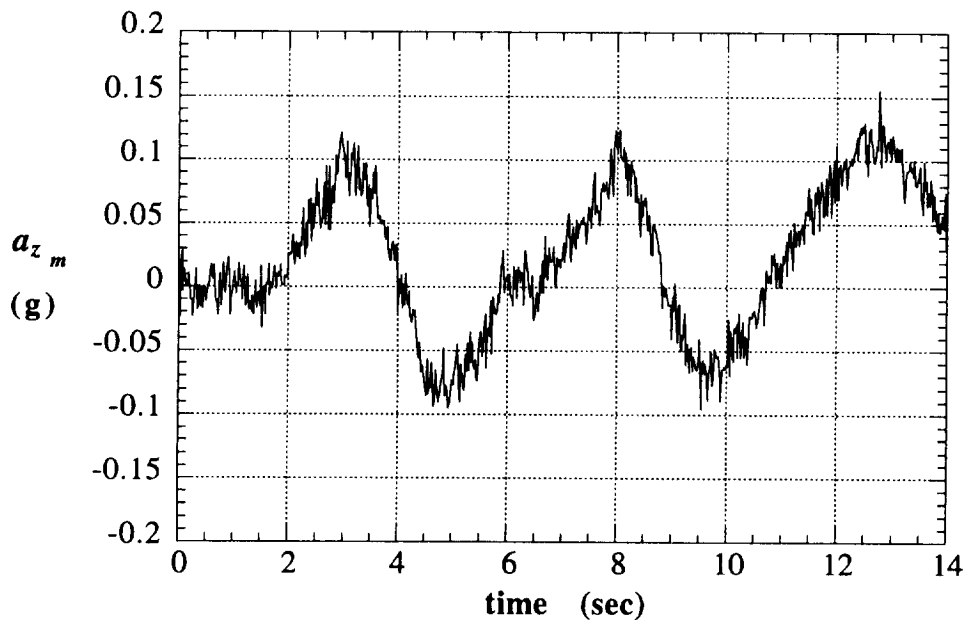


**Figure 2(c)** Simulated vertical acceleration with white measurement noise
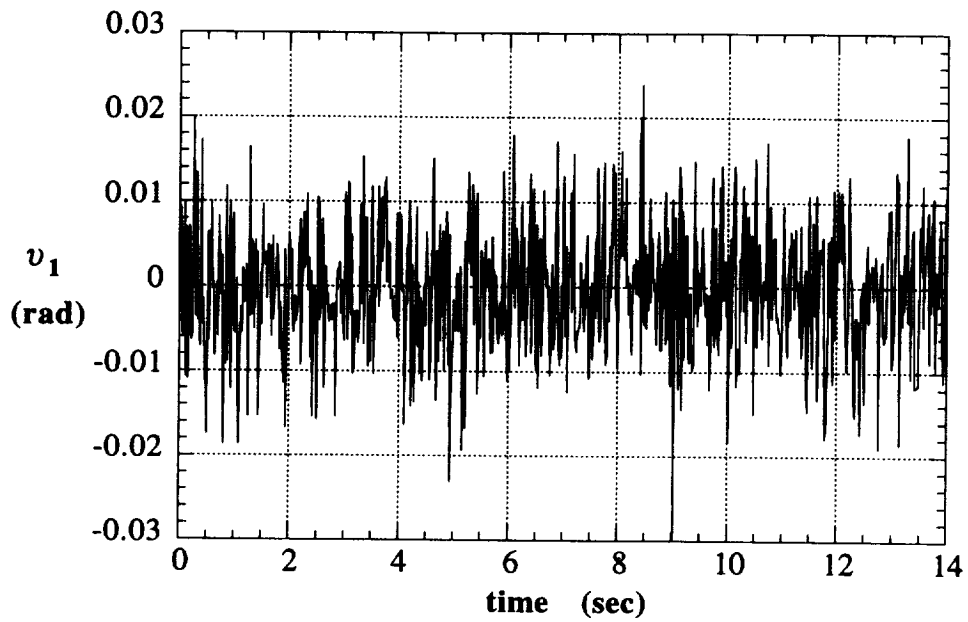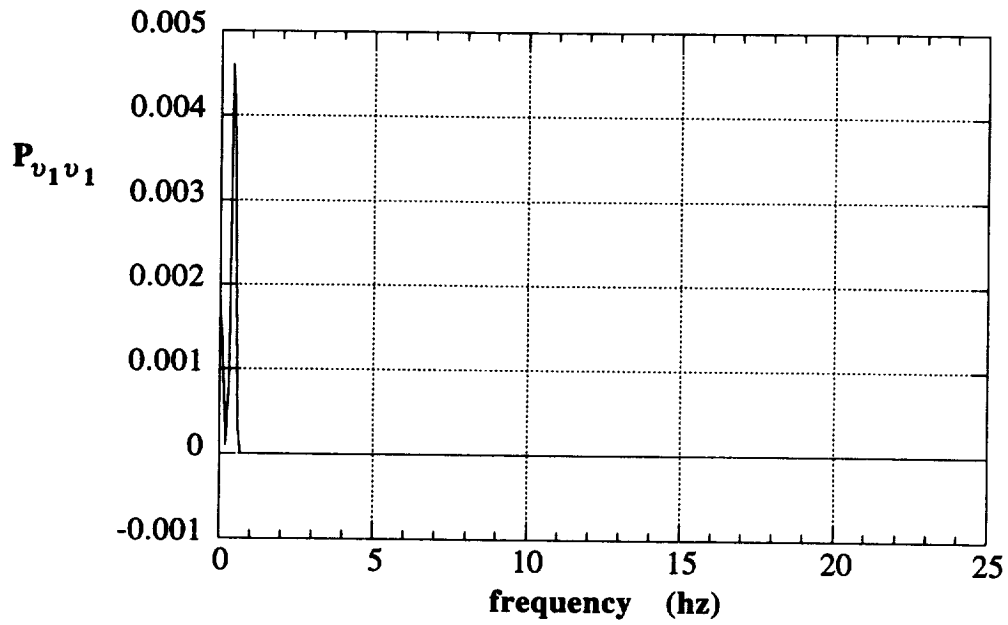
**Figure 3** White noise sequence added to angle of attack
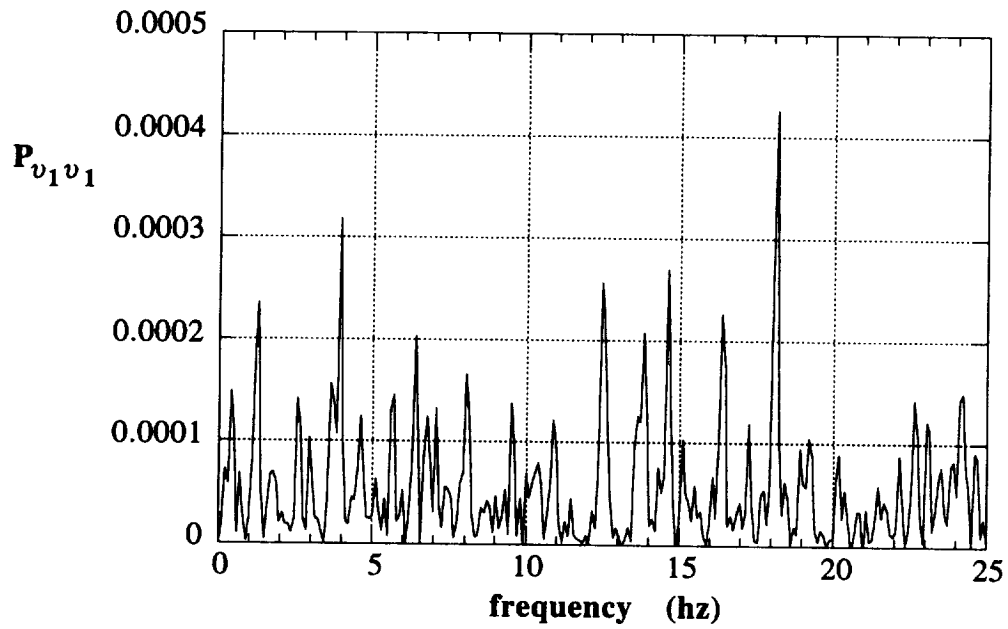


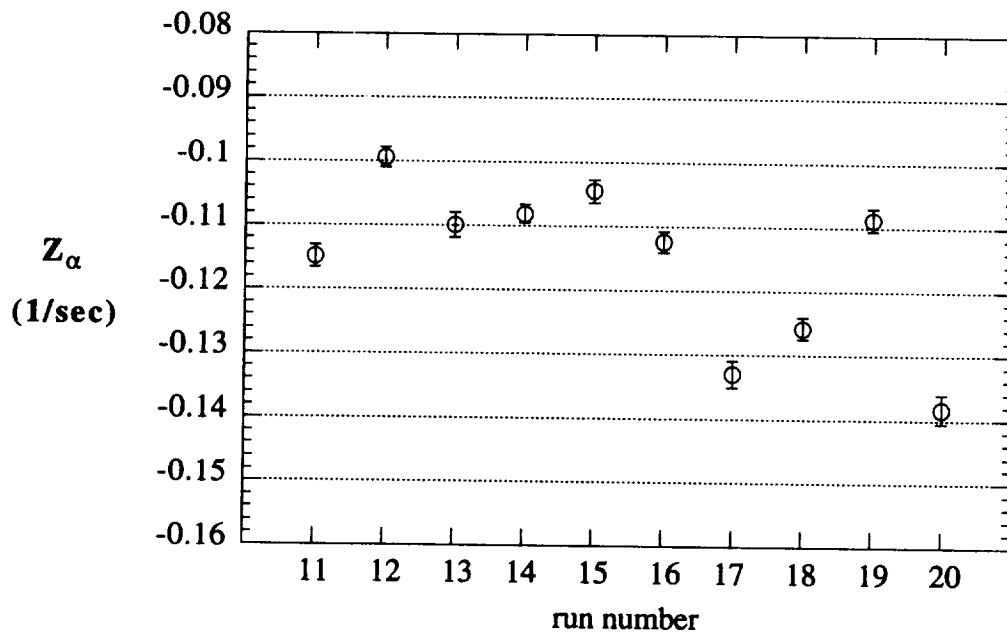**Figure 4** Power spectrum of white noise added to angle of attack
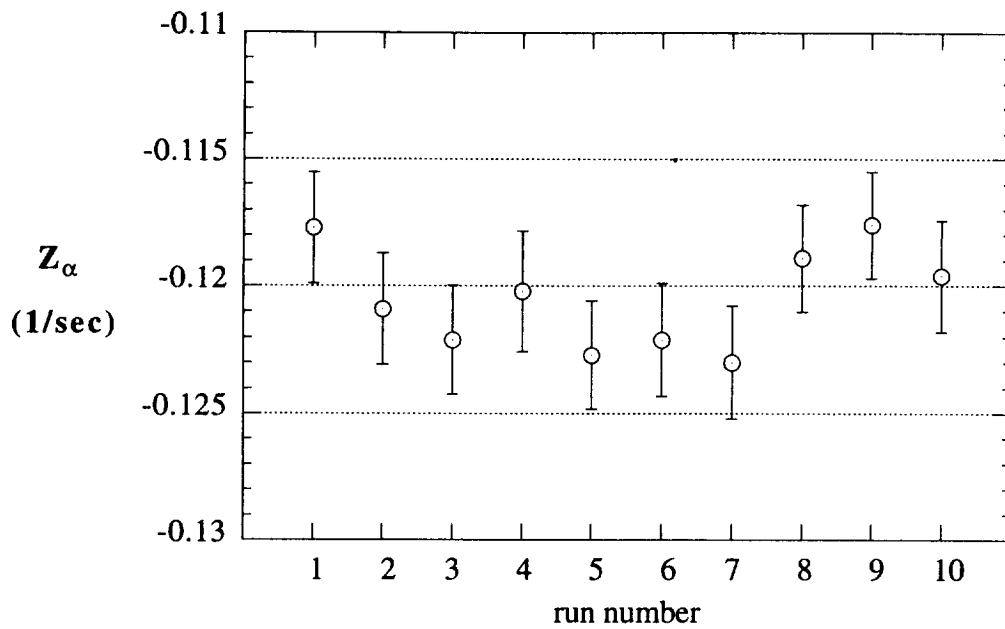
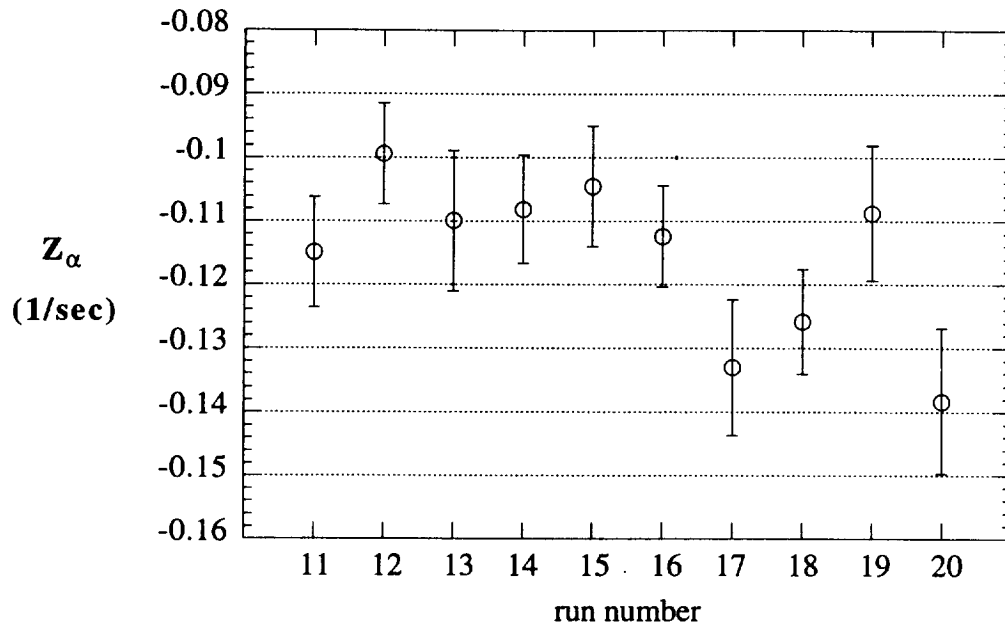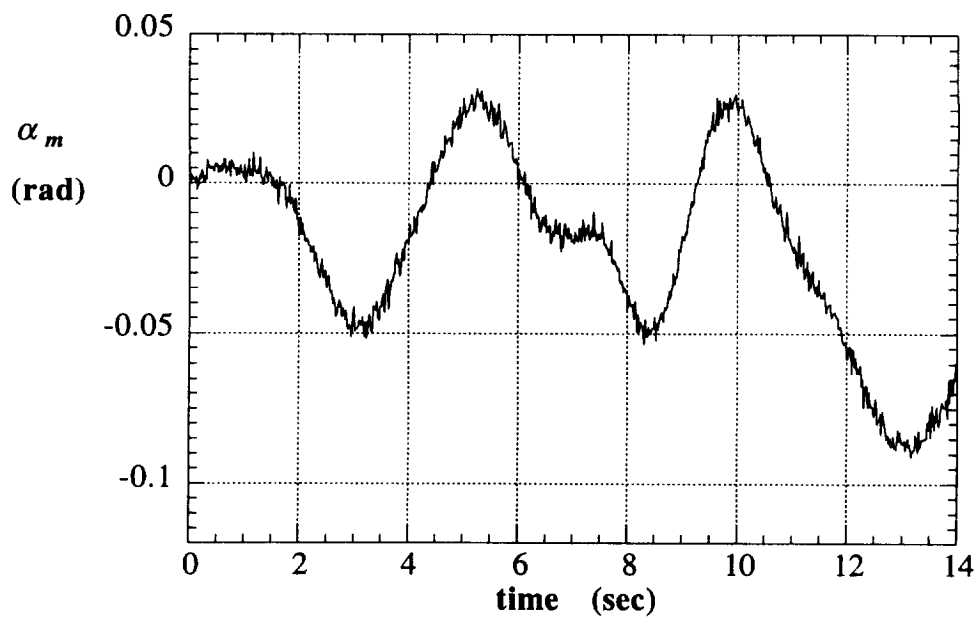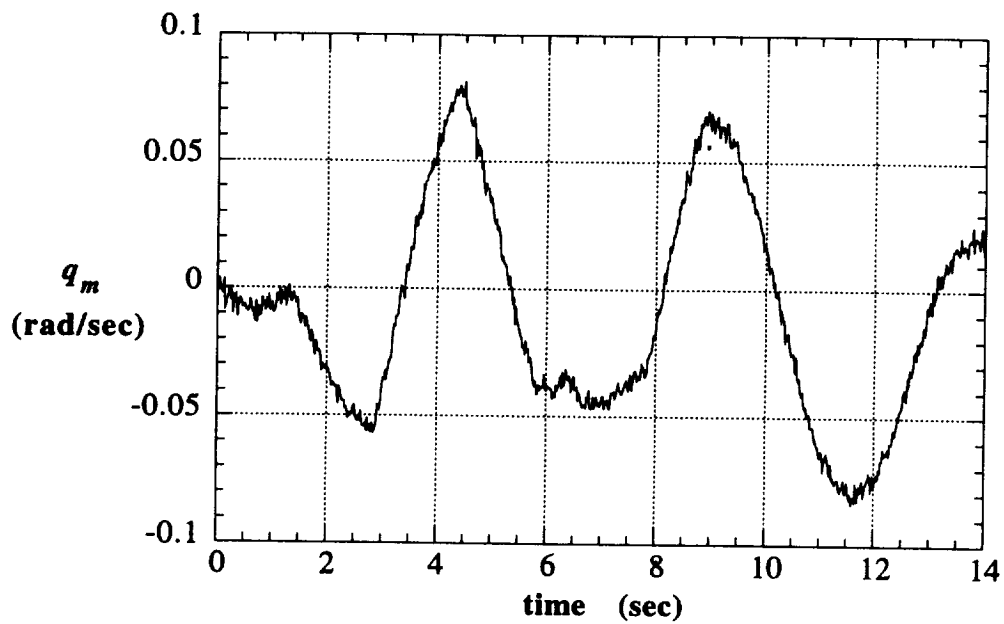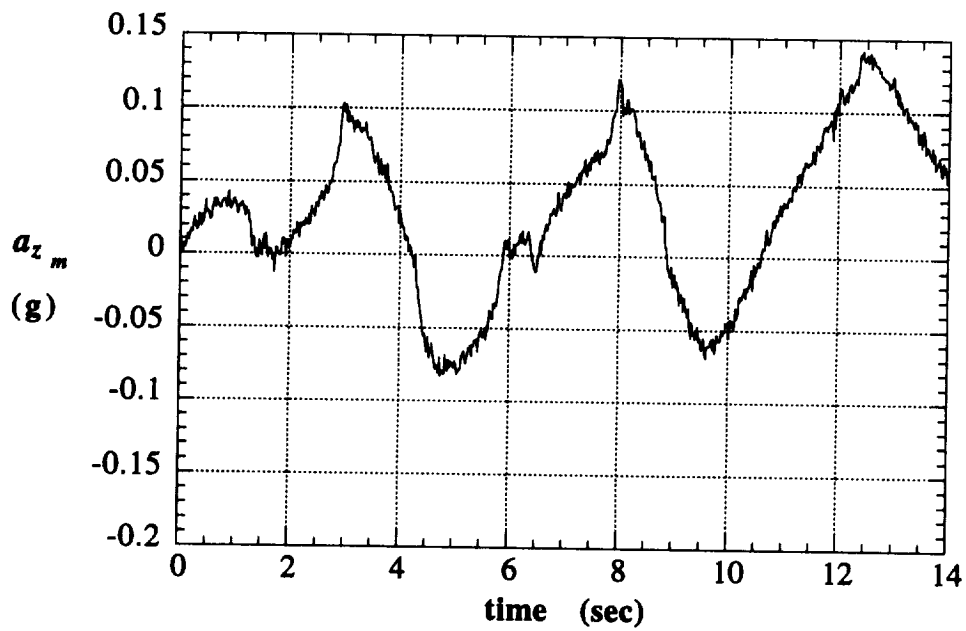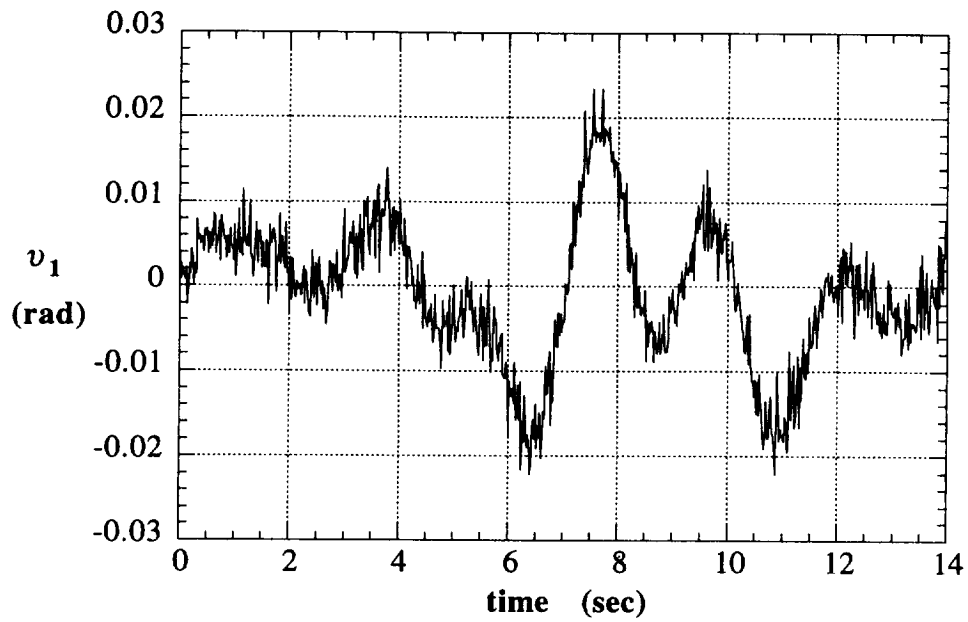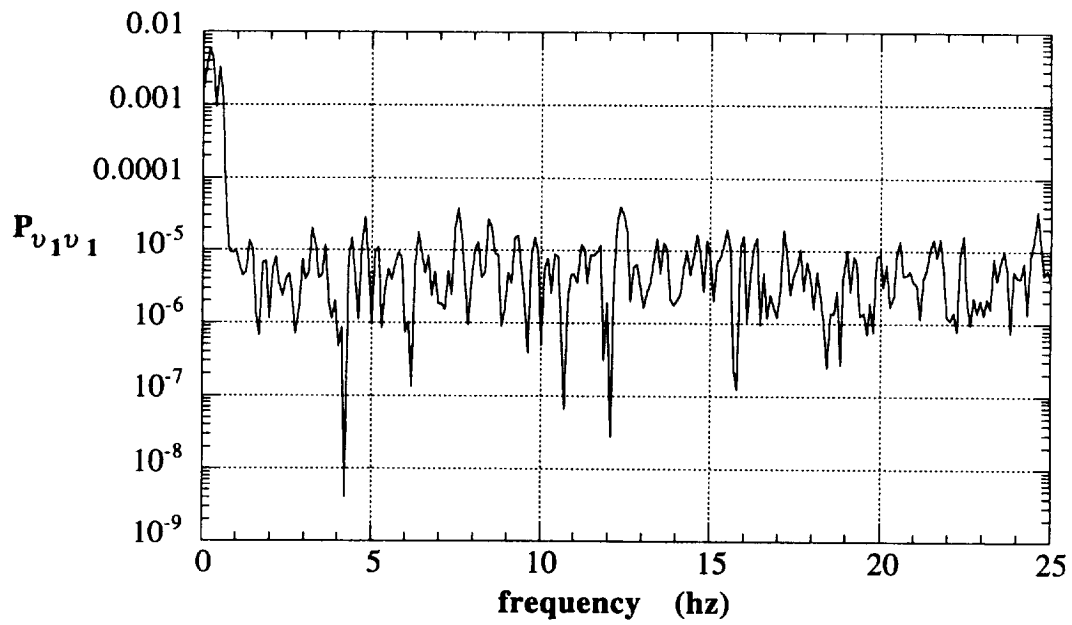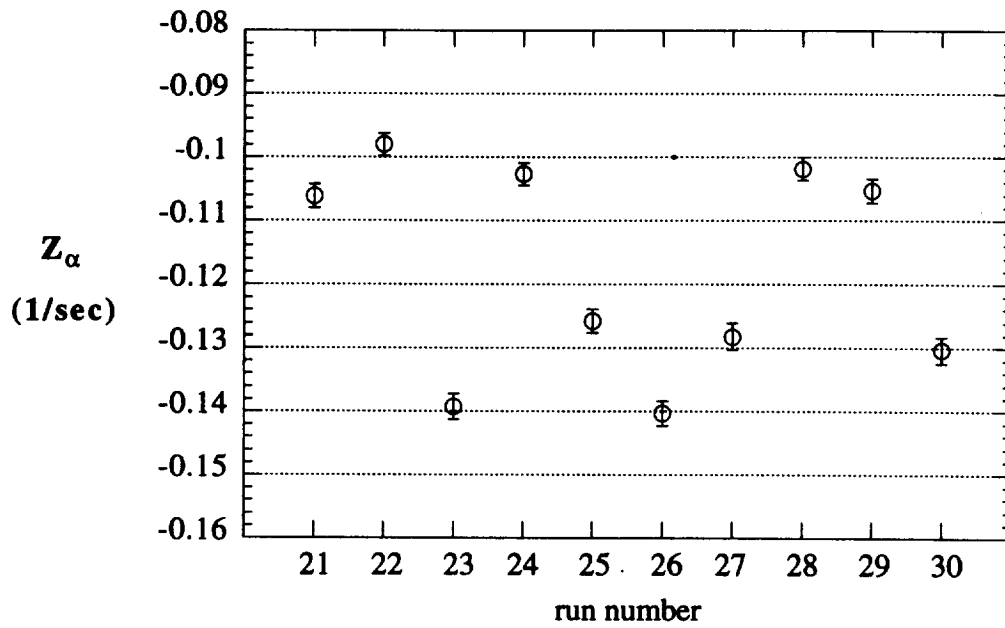**Figure 5** $Z_\alpha$ parameter estimates with standard Cramer-Rao bounds for white noise
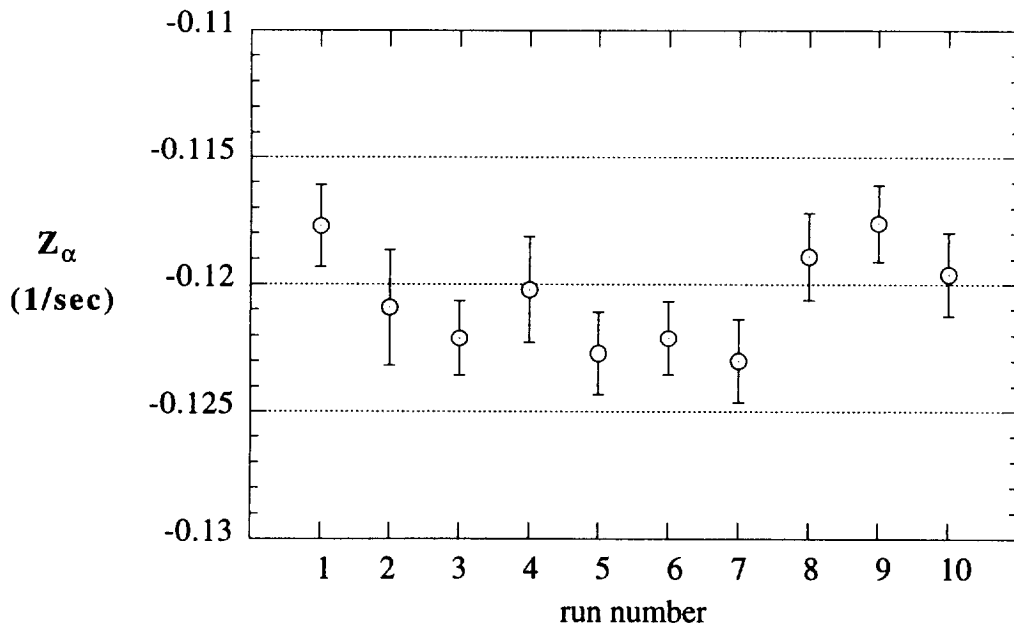


**Figure 6** $Z_\alpha$ parameter estimates with corrected Cramer-Rao bounds for white noise
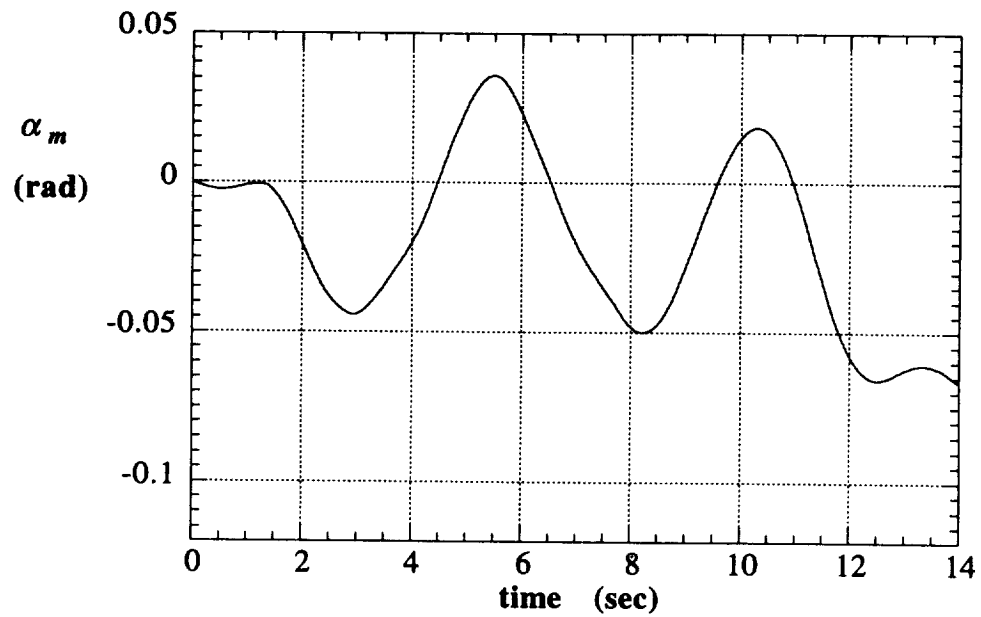
**Figure 7(a)** Simulated angle of attack with band limited measurement noise
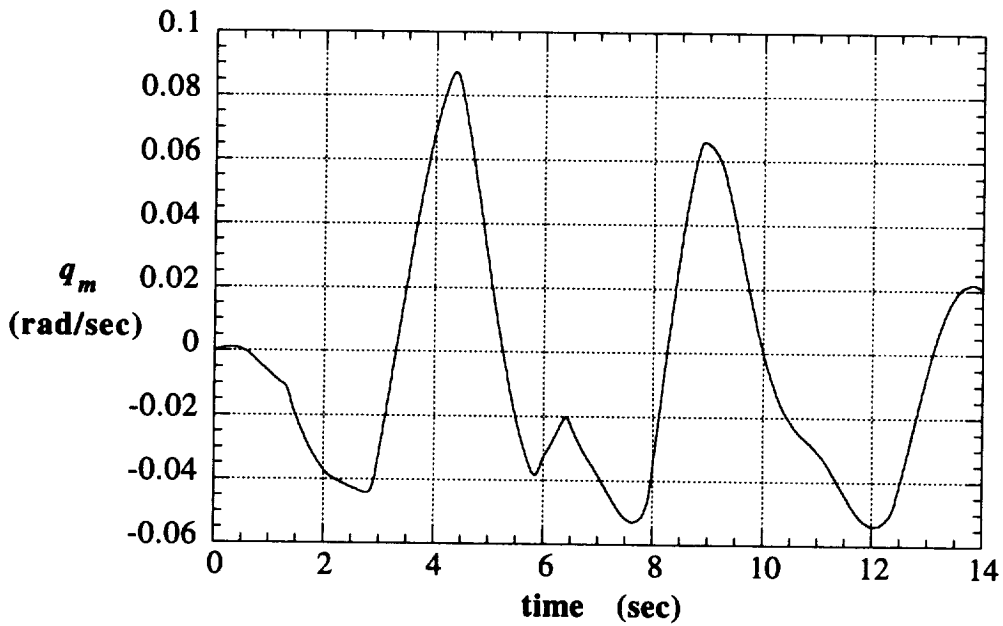


**Figure 7(b)** Simulated pitch rate with band limited measurement noise

40
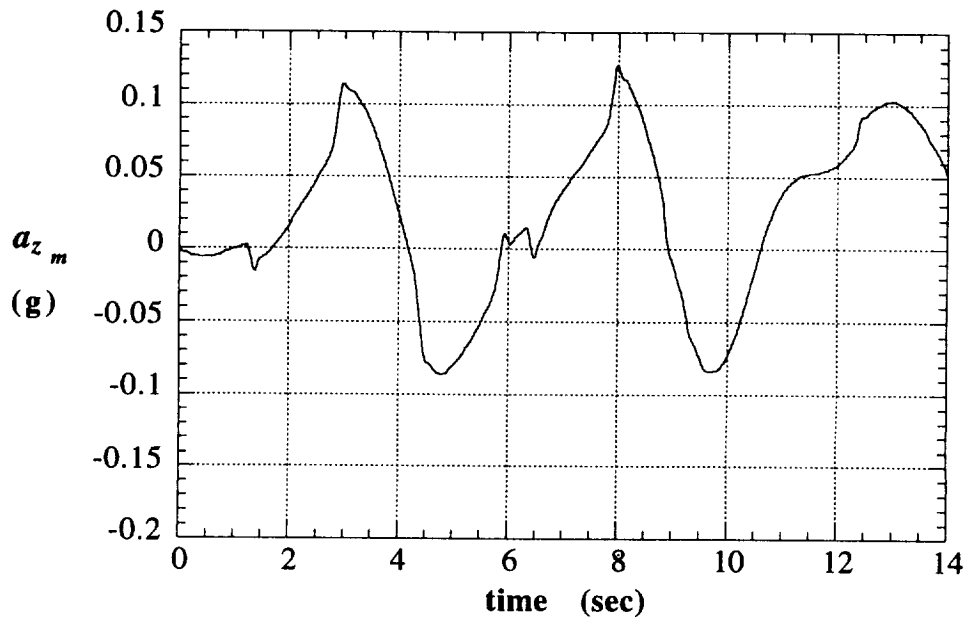
**Figure 7(c)** Simulated vertical acceleration with band limited measurement noise
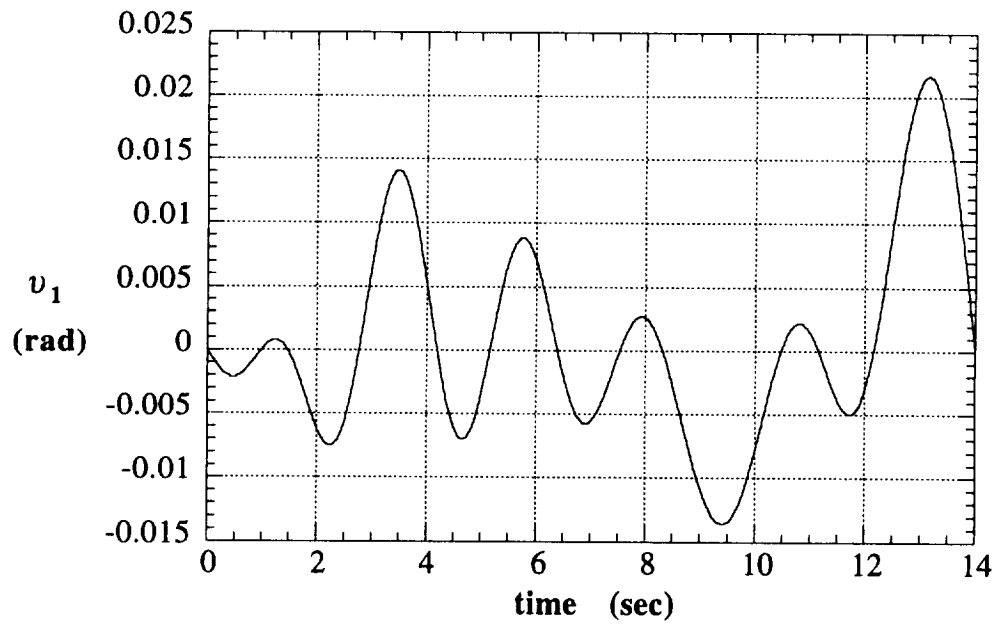


**Figure 8** Band limited noise sequence added to angle of attack

41

**Figure 9** Power spectrum of band limited noise added to angle of attack



**Figure 10** $Z_\alpha$ parameter estimates with standard Cramer-Rao bounds for band limited noise

**Figure 11** $Z_\alpha$ parameter estimates with corrected Cramer-Rao bounds for band limited noise



**Figure 12(a)** Simulated angle of attack with colored measurement noise

43

**Figure 12(b)** Simulated pitch rate with colored measurement noise



**Figure 12(c)** Simulated vertical acceleration with colored measurement noise

**Figure 13** Colored noise sequence added to angle of attack



**Figure 14** Power spectrum of colored noise added to angle of attack

45

**Figure 15** $Z_\alpha$ parameter estimates with standard Cramer-Rao bounds for colored noise
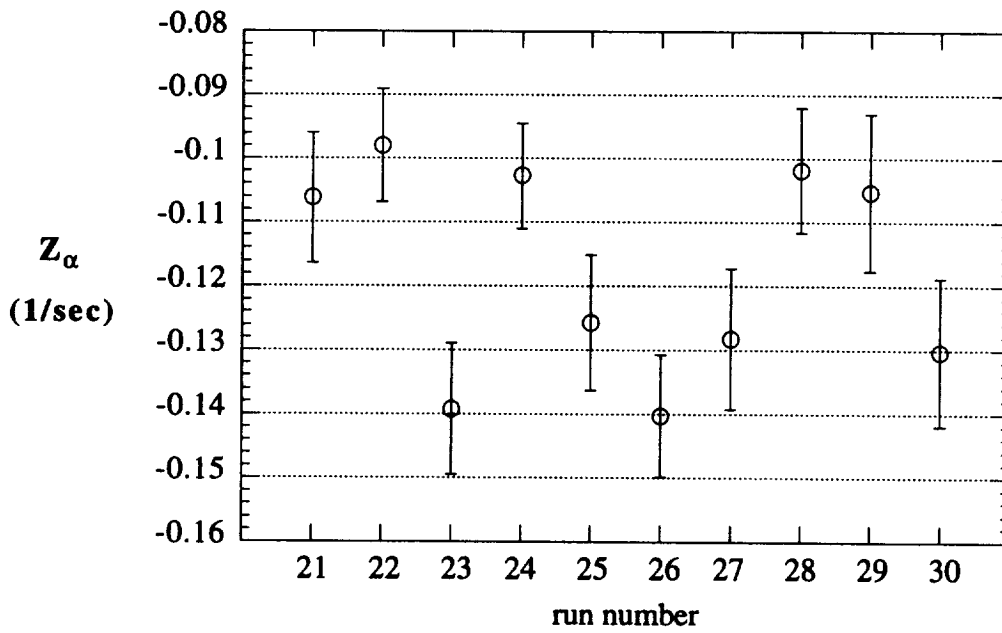


**Figure 16** $Z_\alpha$ parameter estimates with corrected Cramer-Rao bounds for colored noise

# REPORT DOCUMENTATION PAGE

*Form Approved*
*OMB No. 0704-0188*

| 1. AGENCY USE ONLY *(Leave blank)* | 2. REPORT DATE<br>September 1994 | 3. REPORT TYPE AND DATES COVERED<br>Contractor Report |
|---|---|---|

**4. TITLE AND SUBTITLE**

Determining the Accuracy of Maximum Likelihood Parameter Estimates with Colored Residuals

**5. FUNDING NUMBERS**

NAS1-19000
NCC1-29

505-64-30-01

**6. AUTHOR(S)**

Eugene A. Morelli and Vladislav Klein

**7. PERFORMING ORGANIZATION NAME(S) AND ADDRESS(ES)**

Lockheed Engineering & Sciences Company
Hampton, VA 23666 and
The George Washington University, JIAFS
Langley Research Center, Hampton, VA 23681-0001

**8. PERFORMING ORGANIZATION REPORT NUMBER**

**9. SPONSORING / MONITORING AGENCY NAME(S) AND ADDRESS(ES)**

National Aeronautics and Space Administration
Langley Research Center
Hampton, VA 23681-0001

**10. SPONSORING / MONITORING AGENCY REPORT NUMBER**

NASA CR-194893

**11. SUPPLEMENTARY NOTES**

Langley Technical Monitor: Claude R. Keckler

**12a. DISTRIBUTION / AVAILABILITY STATEMENT**

Unclassified - unlimited

Subject category - 08

**12b. DISTRIBUTION CODE**

**13. ABSTRACT *(Maximum 200 words)***

An important part of building high fidelity mathematical models based on measured data is calculating the accuracy associated with statistical estimates of the model parameters. Indeed, without some idea of the accuracy of parameter estimates, the estimates themselves have limited value. In this work, an expression based on theoretical analysis was developed to properly compute parameter accuracy measures for maximum likelihood estimates with colored residuals. This result is important because experience from the analysis of measured data reveals that the residuals from maximum likelihood estimation are almost always colored. The calculations involved can be appended to conventional maximum likelihood estimation algorithms. Simulated data runs were used to show that the parameter accuracy measures computed with this technique accurately reflect the quality of the parameter estimates from maximum likelihood estimation without the need for analysis of the output residuals in the frequency domain or heuristically determined multiplication factors. The result is general, although the application studied here is maximum likelihood estimation of aerodynamic model parameters from flight test data.

**14. SUBJECT TERMS**

Parameter accuracy, maximum likelihood, Cramer-Rao bound, parameter estimation, colored noise

**15. NUMBER OF PAGES**

47

**16. PRICE CODE**

A03

| 17. SECURITY CLASSIFICATION OF REPORT | 18. SECURITY CLASSIFICATION OF THIS PAGE | 19. SECURITY CLASSIFICATION OF ABSTRACT | 20. LIMITATION OF ABSTRACT |
|---|---|---|---|
| unclassified | unclassified | unclassified | |